GEOGRAPHICAL INFORMATION SYSTEM BASED ANALYSIS OF PALEOFLUVIAL SYSTEMS IN THE KUWAIT REGION

By

Redha Mohammad

B.S. in Geological Sciences, University of Oregon, 2002

B.S. in Environmental Sciences, University of Oregon, 2002

Submitted to the Graduate Faculty of

Arts and Sciences in partial fulfillment

of the requirements for the degree of

Masters of Science in Geology

University of Pittsburgh

2008

UNIVERSITY OF PITTSBURGH
SCHOOL OF ARTS AND SCIENCES

This thesis was presented

by

Redha Mohammad

It was defended on

April 17, 2008

and approved by

William Harbert, PhD, Associate Professor

Mark Abbott, PhD, Associate Professor

Michael Rosenmeier, PhD, Associate Professor

Thesis Director: William Harbert, PhD, Associate Professor

GEOGRAPHICAL INFORMATION SYSTEM BASED ANALYSIS OF PALEOFLUVIAL SYSTEM IN THE KUWAIT REGION

Redha Mohammad, M.S.
University of Pittsburgh, 2008

In this thesis, hydrologic mapping and modeling of valley networks using Landsat 7 resolution images and SRTM (Shuttle Radar Topography Mission) derived topographic data are used to quantitatively characterize surface fluvial systems. These stream network models are then used to analyze the role of water in the evolution of the Kuwait region. SRTM-derived Digital Elevation Models (DEM) were combined to build a regional DEM mosaic for the Kuwait region, which was the basis for this analysis. This dataset was analyzed using surface hydrological analysis tools within ArcGIS 9.1 to calculate and model drainage basin geometry and surface stream networks in order to determine basin and network parameters for this region. Stream Order was determined for our stream network model using the Strahler method of ordering. In the study region, a well developed stream network ranging from first to fifth Strahler orders was identified and modeled, defining regions for future investigation of paleochannels created during a paleo climatic wetter period. This model indicates spatial regions within which further research and field investigation are required to analyze the sedimentary deposits in these modeled streams to identify the mechanism and environment of formation.

TABLE OF CONTENTS

LIST OF TABLES

LIST OF FIGURES

ACKNOWLEDGMENTS

I would like to thank my beloved mother, who believed in me when I didn't believe in myself, who supported me and made my success her priority in life, and made every effort to make it possible for me to come to the United States and pursue my dream of attending graduate school.

I would also like to thank my academic advisor, Professor William Harbert, whose guidance and tremendous help have made this work possible, especially at times when everything seemed to be going in the wrong direction.

Finally, I would like to thank Ian Kramer from ESRI for his support and valuable time.

1.0 INTRODUCTION

1.1 Study Goals

The goal of this study is to utilize the spatial, surface and network tools of Geographical Information Systems (GIS), specifically the hydrologic tools of ArcHydro, to determine, model and analyze possible paleochannels that were formed in the Kuwait region of northeastern Arabia. Paleochannels would have formed during periods of increased precipitation, either due to an increase in the monsoon summer rain or an intensification of winter-driven rainfall. The results of this GIS-based study should aid further field studies, specifically through identification of key sites for further sediment studies and reconstructions of paleoclimatic conditions.

1.2 Large-Scale Climate Change

Changes in climate can occur rapidly as a result of sudden events, such as large-scale volcanic eruptions or a meteor impact. These changes are typically short-term and result from variation in feedback systems and last between weeks to few years (Ruddiman, 2001). In contrast, long-term changes in climate occur gradually over tens to hundreds of thousands of years. These long-term changes are referred to as orbital-scale climate changes as they are caused by changes in earth's orbit. They include changes in earth's eccentricity, obliquity, and precession index (Hecht, 1985). These changes, in part, control the amount of solar radiation received by earth, and consequently cause large-scale climate change (Ruddiman, 2001). Changes in insolation receipt seem to occur in cycles of 23,000, 41,000, and 100,000 years. Evidence from lake deposits in Africa

suggests that lake levels across tropical and subtropical North Africa were at much higher levels around 9,000 years ago when summer insolation was 8% higher than today (Ruddiman, 2001). The peak in summer insolation is believed to have occurred 10,000 and 9,000 years ago (Kutzbach, 1981), indicating a correlation between increased summer insolation and increased monsoonal rain (Fig.1). Therefore, it is believed that solar radiation was greatest 6-12,000 years ago, with its maximum around 9,000 years ago (Paeth, 1999).

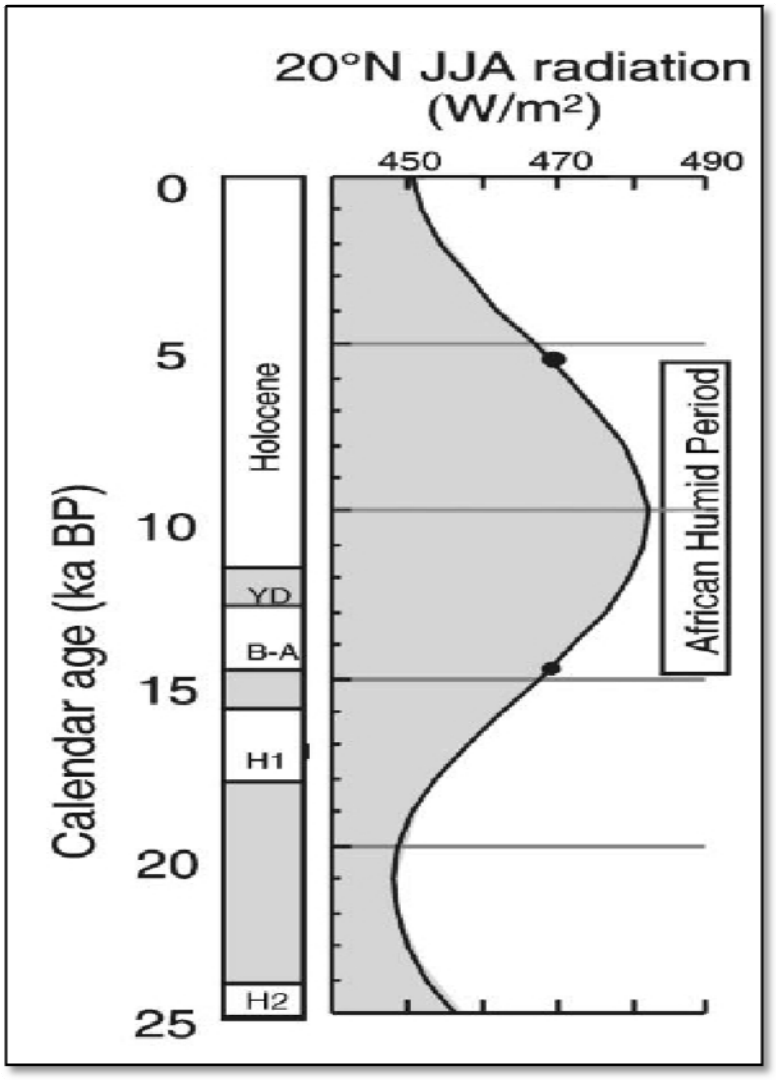

Figure 1. Conceptual model of the monsoon's response to changes in summer insolation (Watts per Sq. meter) at 20˚ N in North Africa. Increases in summer insolation heating to values above a critical threshold appear to have driven a stronger African monsoon around 10,000 yrs ago (deMenocal *et al*, 2000).

1.3 Paleoclimate

Paleoclimatic Information can be obtained from climate archives or proxies. They include marine and lake sediment deposits, ice cores, corals, oxygen isotope, pollen data, and tree rings (Hecht, 1985). Other methods include measuring concentrations of atmospheric noble gases (neon, argon, krypton, and xenon) dissolved in groundwater (Weyhenmeyer *et al*, 2000). Long-term (millions of years) climate changes are represented best in sedimentary layers, especially in uninterrupted sedimentary sequences along continental margins. They form when rainfall and its runoff erode exposed continental rocks and transport eroded sediments in streams and rivers. These sediments are eventually deposited in layers. Runoff created by rainfall also transports sediments and dissolved minerals that eventually flow into the ocean and become part of the oceanic floor depositional layers. Oceanic cores have a resolution of 10,000 to 10 million years, with the highest resolution averaging between 100,000 and 200,000 years (Hecht, 1985).

1.4 Paleofluvial Systems

Topography, surface geology, and climate are the key factors controlling the pattern, size, and geometry of drainage networks (Al-Sulaimi, 1997). The geometry and structure of drainage networks are also a key indication of climate. Climatic conditions, particularly the rate and pattern of precipitation, are responsible for the initiation and maintenance of drainage networks through surface runoff erosion and carving of exposed rocks and sediments (Al-Sulaimi, 1997). Geologic classifications of streams include influent, effluent, and intermittent streams (Fig.2). Influent streams provide water to the ground

water storage. Effluent streams, also referred to as Perennial streams, convey water from ground water storage year round (Black, 1991).

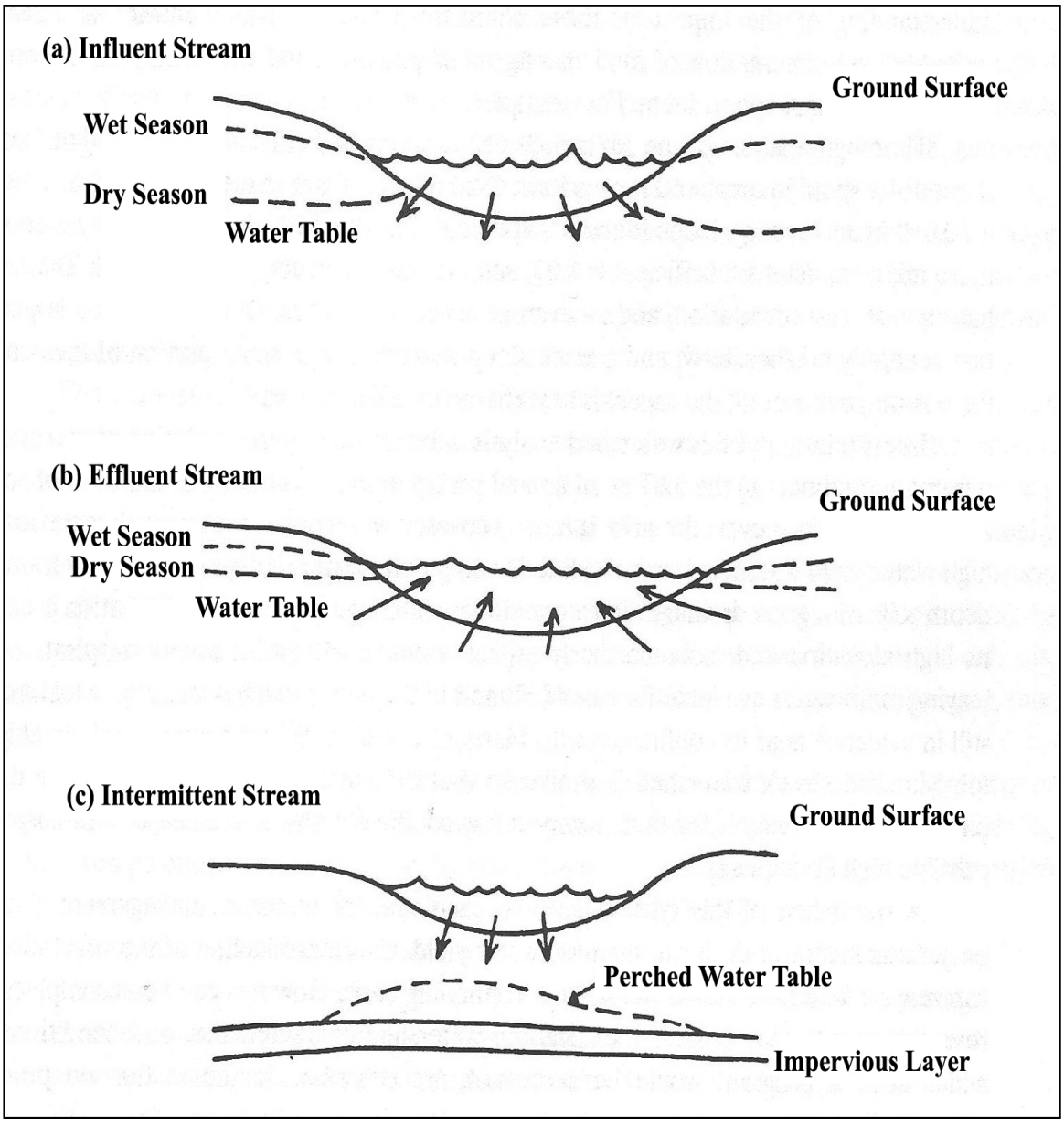

Figure 2. Geologic classification of streams (Black, 1991).

In arid climates and following a runoff-causing event, ephemeral streams flow for a short period before drying up rapidly due to the high infiltration rate into the unsaturated zone beneath the streambed or by evaporation (Black, 1991). Ephemeral streams are therefore seasonal streams that are initiated by rainfall events. Intermittent streams, which may also flow immediately following a runoff-causing event, provide water to a perched water table or to deep seepage (Black, 1991). This type of streams is usually permanent, although prolonged periods of drought can cause an intermittent stream to dry up and cease flowing.

Due to the extremely low precipitation rates and its sporadic nature in deserts, vegetation is generally very sparse. Consequently, when precipitation occurs, it tends to create flash floods. Rainwater typically drains towards the centers of desert basins, where playas or inland sabkhas may develop and become sites of deposition of carbonate and evaporite minerals (Boggs, 2006).

Despite the current arid conditions in the Kuwaiti desert, its northern part has well-developed drainage networks that can be identified from satellite images. A study by Al-Sulaimi et al. (1997) concluded that this well-developed drainage network (Fig.7) required a high rate of surface runoff that transported sediments and eroded the surface. These authors also concluded that such conditions could only exist in regions with high precipitation, low evaporation, and limited vegetation cover. This suggests that the drainage network in northern Kuwait was developed during a pluvial episode dominated by fluvial geomorphological processes.

2.0 STUDY AREA DESCRIPTION

2.1 Present Day Climate of Arabia and Kuwait

Tropical heating causes air to rise in the tropics, flow to the subtropics, sink near 30˚ latitude, then flow back toward the tropics as surface trade winds. In the troposphere, the atmospheric layer immediately above the earth's surface, the atmospheric circulation cell is called a Hadley Cell (Fig.3) (Ruddiman, 2001).

Today, the Arabian Peninsula lies in a subtropical zone where climate is shaped by the cool dry air descending from the Hadley Cell. Consequently, most of Arabia has low precipitation and an average annual rainfall of less than 100 mm (Edgell, 2006). Summer temperatures average 42-45°C in central Arabia and may exceed 50°C in the interior deserts. In contrast, winter temperatures can drop below freezing at night and early morning, although daytime temperatures usually remain in the 10-20°C range.

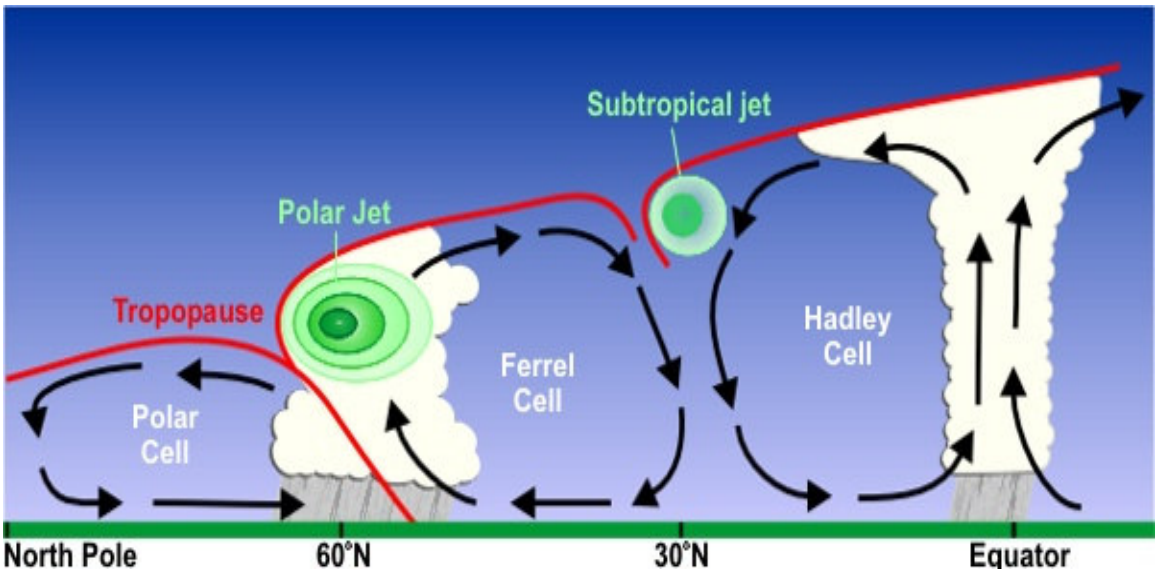

Figure 3. As air heats and rises in the tropics, it creates rain along the tropics then loses moisture and sinks as dry air in the subtropics, creating a Hadley cell flow (http://www.srh.noaa.gov/jetstream//global/images/jetstream3.jpg).

In Kuwait, climate is characterized by long, hot, and dry summers. The annual mean rainfall value is ~105 mm, with minimum and maximum recorded values of 23 and 242 mm respectively. Precipitation occurs mainly between the months of November through April. The average number of rainy days per year is 28.1. Annual mean potential evapotranspiration totals nearly 2300 mm, well over 20 times the annual mean precipitation (Al-Sulaimi et al., 1997). Average annual temperature ranges from 7.8 °C in January to 44.6°C in August. Table 1 and Figure 4 show average monthly maximum and minimum temperatures and rainfall means.

Average	*Jan*	*Feb*	*Mar*	*Apr*	*May*	*Jun*	*Jul*	*Aug*	*Sep*	*Oct*	*Nov*	*Dec*
Precipitation (mm)	6.0	3.8	4.5	3.7	1.8	0.0	0.0	0.0	0.0	0.7	3.1	4.5
Max Temp (C˚)	18	21	26	31	38	43	44	45	42	35	26	19
Min Temp (C˚)	7	9	13	18	24	27	29	28	24	19	13	8

Table 1. Average monthly maximum and minimum temperatures and rainfall means in Kuwait (Al-Sulaimi et al., 1997)

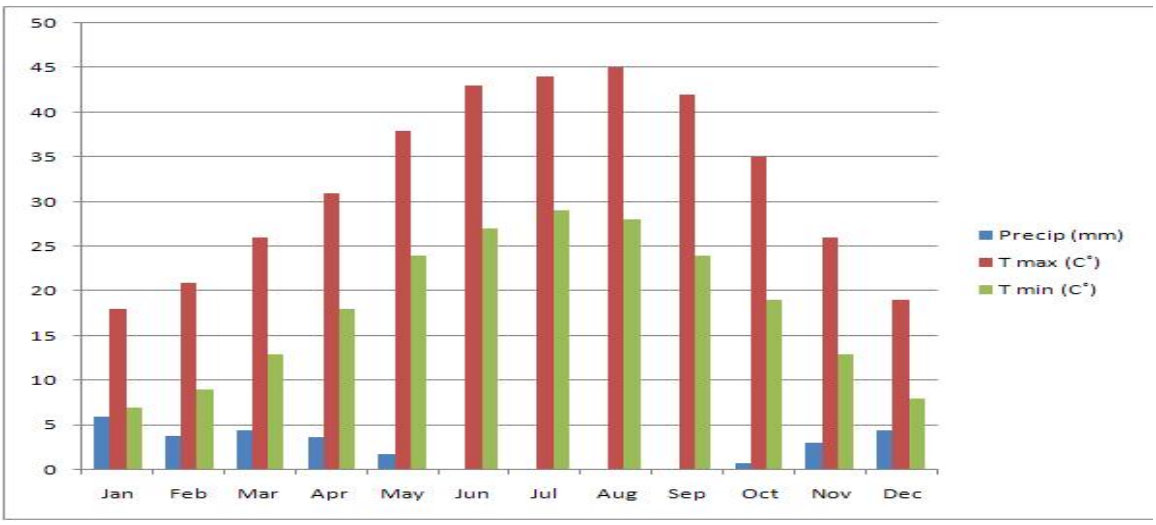

Figure 4. Average monthly maximum and minimum temperatures and rainfall means in Kuwait (Al-Sulaimi et al., 1997)

2.2 Geological Setting

Kuwait is located between the Arabian Shield and the Zagros fold belt at the periphery of the Arabian platform (Fig.5). Arabia formed during the Paleozoic, initially as a low-lying northeastern corner of Africa, with the shallow seaway of the Tethys lapping onto its northeastern margin (Edgell, 2006). Marine sediments that were predominantly of shallow water origin were deposited in this gently subsiding seaway from Cambrian-Ordovician to the Early Tertiary, with sporadic periods of non-deposition occurring occasionally (Edgell, 2006). During the Oligocene, Arabia began to split away from Africa with great uplifts on either side of a fissure that developed into the Red Sea. Arabia then became a separate tectonic plate. Today, the Arabian Plate is moving north-east at rates now estimated from GPS measurements to be 25 mm/year for Oman or 15.7 mm/year for the southern Red Sea (Edgell, 2006). As a result of the Arabian Plate's northward movement and collision with the Eurasian Plate, the Iranian Plate has been

under-ridden by the subduction of the Arabian Plate, causing the uplift of the Zagros and Taurus mountain ranges (Edgell, 2006).

Rock units exposed within range in age from Eocene to Holocene. The landscape in Kuwait is predominantly carved in friable to partially cemented clastic deposits of Miocene to Pleistocene age locally known as the Kuwait Group, which unconformably overlies the Middle Eocene dolomite-limestone of the Dammam Formation and varies in thickness between 390 m in the northeast to only 8 m in the southeast of Kuwait (Al-Sulaimi et al., 1997).

The Kuwait Group is divided into three formations: The Ghar, Fars, and Dibdibba Formations.

The Ghar and Fars formations mostly consist of poorly sorted muddy sandstone rich in granules with sporadic intercalations of sand, mud, and pebbly gravel lenses. This sequence has been subjected to several episodes of calcretization (Al-Sulaimi, 1997).

The Dibdibba Formation (Fig. 6) is the largest occurrence of Quaternary gravel in Arabia and covers most of northern area of Kuwait. The lower member of this formation is widely exposed in the west and north-central Kuwait and consists of brown-weathered medium to very coarse grained gritty and pebbly calcretic sandstones. The upper member of the Debdibba Formation underlies the extensive undulating plain of north and northeast Kuwait and extends towards the southwest as copings to the sinuous ridges characteristic of the northwestern area of Kuwait. It consists of fluviatile sequence of ungraded, often cross-bedded sands and gravels with subordinate intercalcations of sandy mud (Al-Sulaimi, 2000).

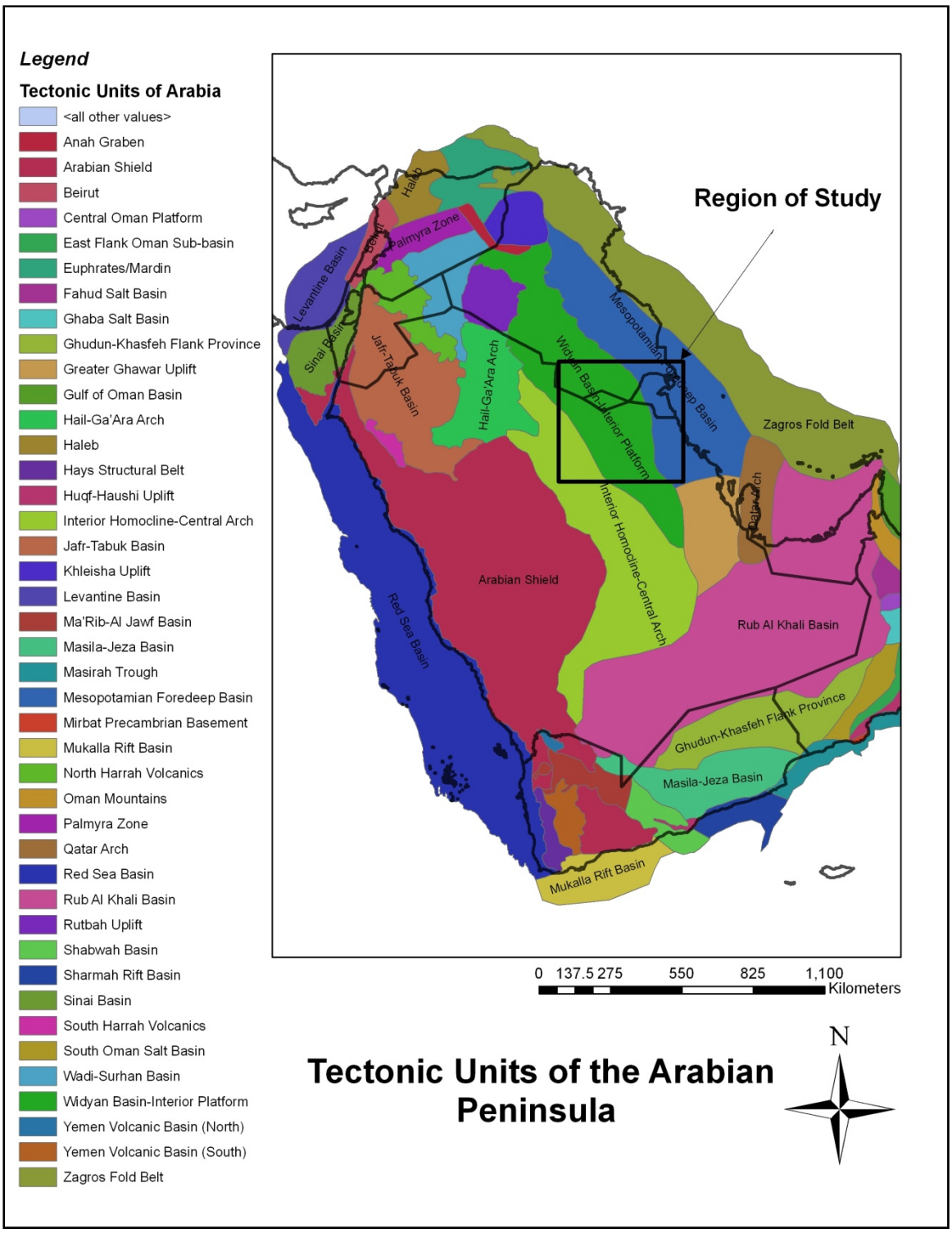

Figure 5. Location of Kuwait between the Arabian Shield and the Zagros fold belt (Al-Sulaimi et al., 2000)

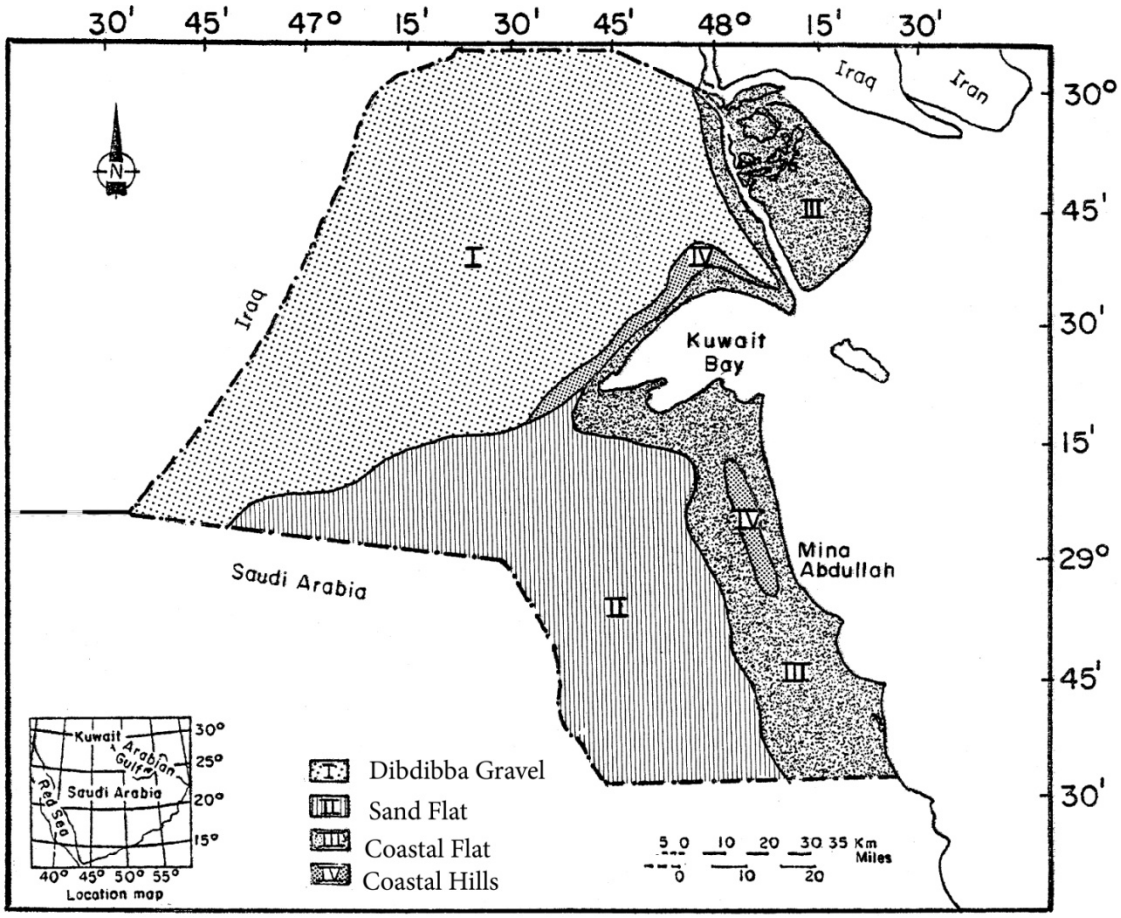

Figure 6. The three formations of the Kuwait Group (Hunting Geology and Geophysics, 1981)

Two areas in the northern and western parts of Kuwait, representing low-lying areas and depressions, are covered by a blanket of desert plain deposits (desert floor). These deposits have been developed as a sheet wash of reworked material from the Dibdibba gravel deposits, most likely during wet periods in the Early Holocene (Al-Sulaimi et al.,1995). These regional formations are ideally suited to record paleo stream drainage networks analysis. Investigation of field sites along these networks would be critical to an improved understanding of variation of climate in this region.

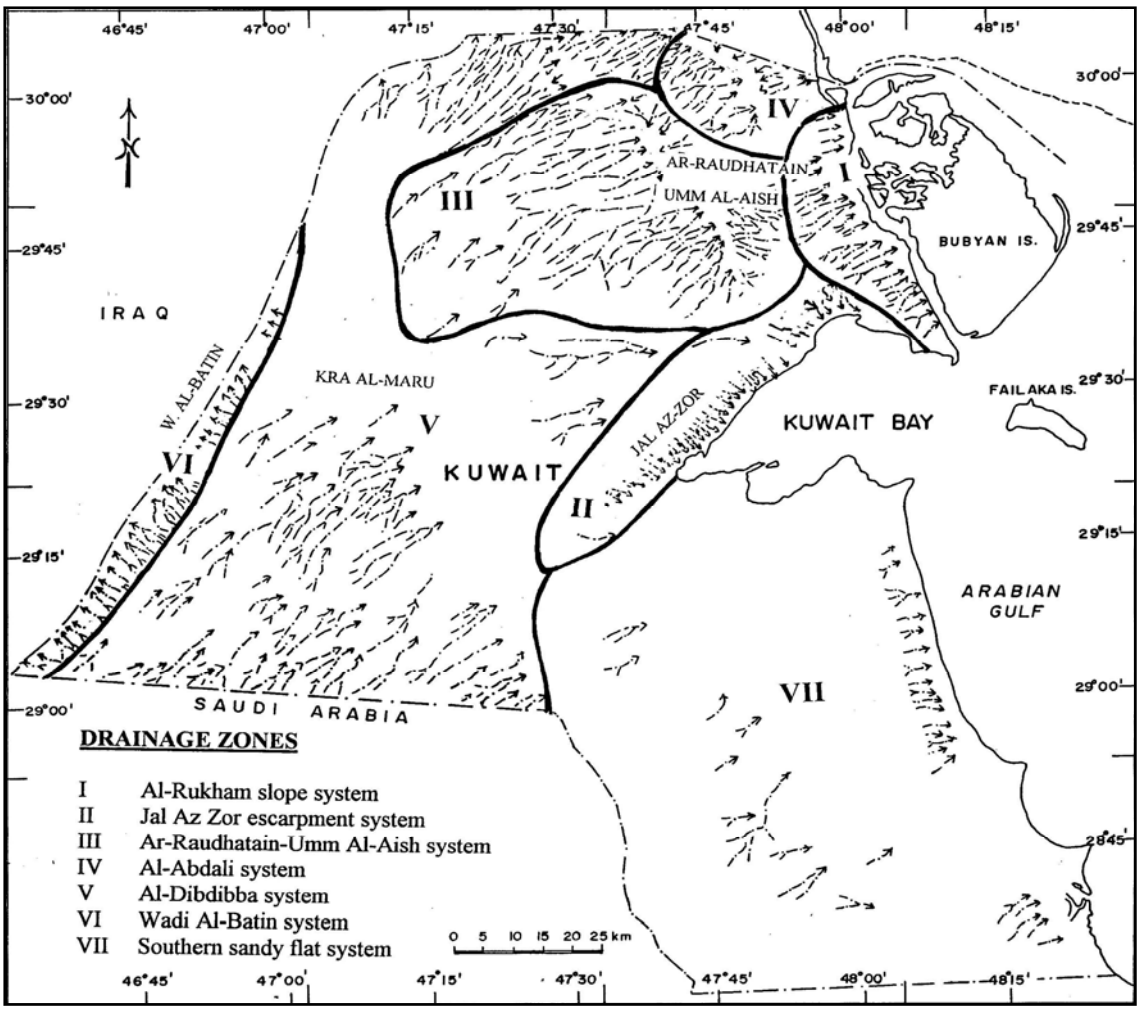

Figure 7. Zones of drainage systems in Kuwait, with arrows representing direction of drainage. Note the incomplete and discontinuous nature of these drainage systems (Al-Sulaimi et al., 1997).

2.3 Present Surface Hydrology of the Area

Today, no streams or rivers exist within Kuwait. Despite the present aridity of the Kuwaiti desert, its northern part has well-developed drainage networks that can be easily recognized from satellite images. A study by Al-Sulaimi et al. (1997) concluded that this well-developed drainage network (Fig.7) required a high rate of surface runoff that transported sediments and eroded the surface. These authors also concluded that such

conditions could only exist in regions with high precipitation, low evaporation, and limited vegetation cover. This suggests that the drainage network in northern Kuwait was developed during a pluvial episode dominated by fluvial geomorphological processes.

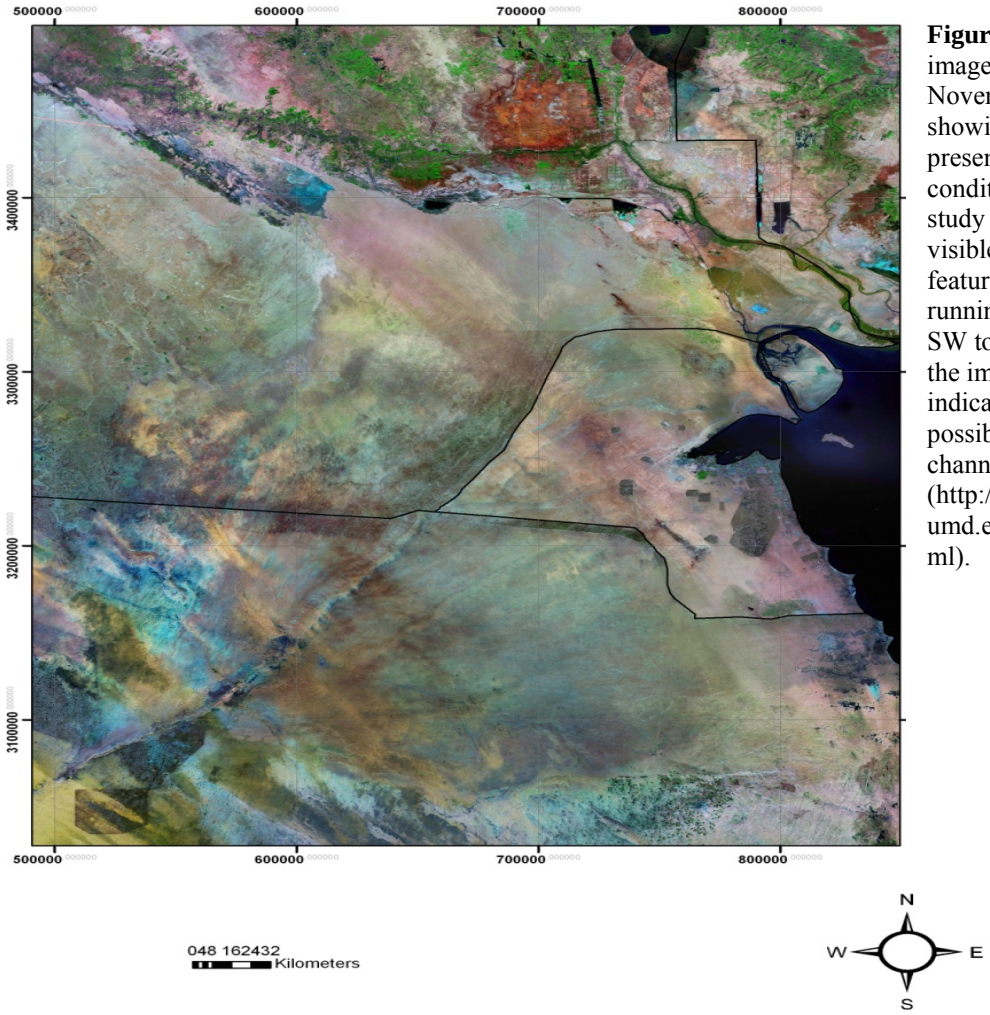

Figure 8. Landsat image taken November 2007 showing the present arid conditions of the study area. A visible channel-like feature can be seen running from the SW to the center of the image, indicating a possible paleo channel (http://glcf.umiacs.umd.edu/index.shtml).

3.0 MONSOONAL VARIABILITY

Much like the Sahara desert, Arabia is situated within a climatically sensitive latitudinal zone of shifting wind belts. Today, the northern part of Arabia (Fig. 9a) receives much of its rainfall during the winter as a result of middle to high-latitude westerly depressions whose tracks are steered by the subtropical jet stream (SJT). In contrast, the southern

part of Arabia (Fig. 9b) receives precipitation largely from summer monsoons (Fischer, 2004). Precipitation in Kuwait occurs during the winter months only (Fig. 4) as a result of its location in the northeastern part of Arabia. The extent of the summer monsoon is limited to areas that are well to the south of Kuwait, and therefore summer monsoons do not affect Kuwait.

Monsoonal climate circulation is the result of strong solar radiation during the summer causing rapid warming of the land but slower and less intense warming of the ocean. Rapid heating over the continents causes air to warm, expand, and rise. This upward movement of warm air creates an area of low pressure over land. Flow of air toward this low-pressure region causes warm, moist air from the oceans to move in. This inflow carries water vapor evaporated from the nearby ocean and contributes to monsoonal rainfall (Ruddiman, 2001). The opposite scenario takes place during the winter, when solar radiation is much weaker and consequently continental air is much cooler and denser.

A widely accepted hypothesis proposed by John Kutzbach in the early 1980's linked changes in insolation to the strength of monsoons over orbital time scales (Fig.10). Periods of increased summer insolation were associated with stronger monsoons and periods of decreased insolation were associated with much weaker monsoons (Ruddiman, 2001). The most recent occurrence of high summer insolation occurred 9,000 years ago (Kutzbach, 1981), and evidence of higher lake levels across tropical and subtropical northern Africa indicate a similar age (Kutzbach, 1985).

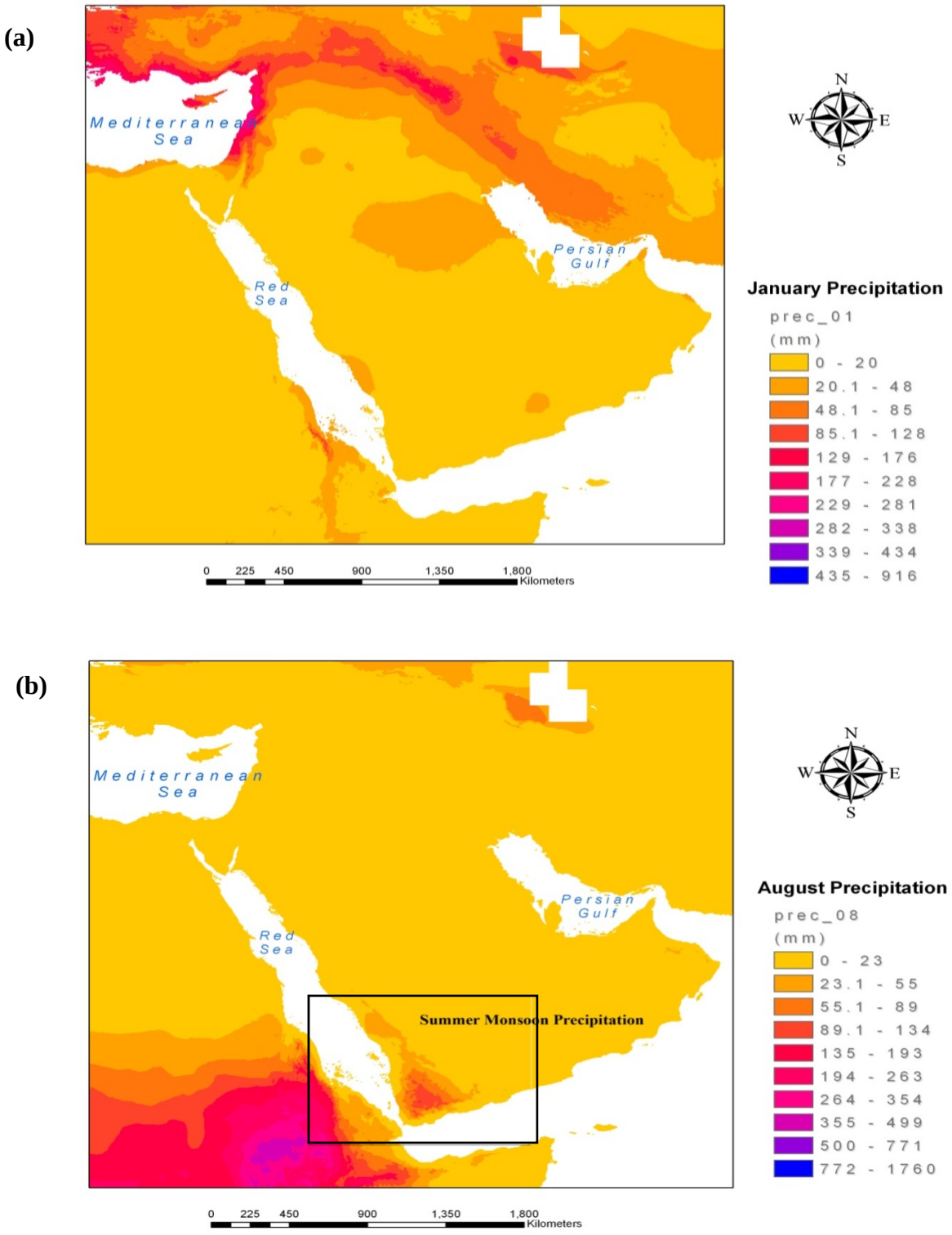

Figure 9. (a) The Northern part of Arabia receives much of its precipitation during the winter months due to high-latitude westerly depressions. (b) The Southern part of Arabia receives much of its precipitation during the summer months as a result of the monsoon (www.worldclim.org)

Sediment deposits in arid regions generally lack organic material and form by eolian or wind-driven processes. On a much smaller scale, fluvial processes may also play a role in sediment deposition in arid regions. Al-Sulaimi et. al (1995) examined two locations in northern and western Kuwait, where low-lying areas and depressions were covered with desert-plain deposits. They concluded that these deposits formed as a sheet wash of reworked material by fluvial processes during a wetter period. Radiocarbon dating of lacustrine deposits from Rub'al Khali (SE Saudi Arabia) suggests that periods of high lake levels occurred between 10.2- 6.8 cal ka (Fischer, 2004). Further north, organic deposits dated to 7.6 cal ka, clustered between eolian deposits, were discovered at Jubba (28°N, 40°56'E), indicating more active fluvial processes and a likely northward extension of the humid climate. However, the effects of the monsoonal precipitation in northern Arabia appear less strong when compared to southern Arabia, indicating a decrease in monsoonal precipitation northward (Fischer, 2004)

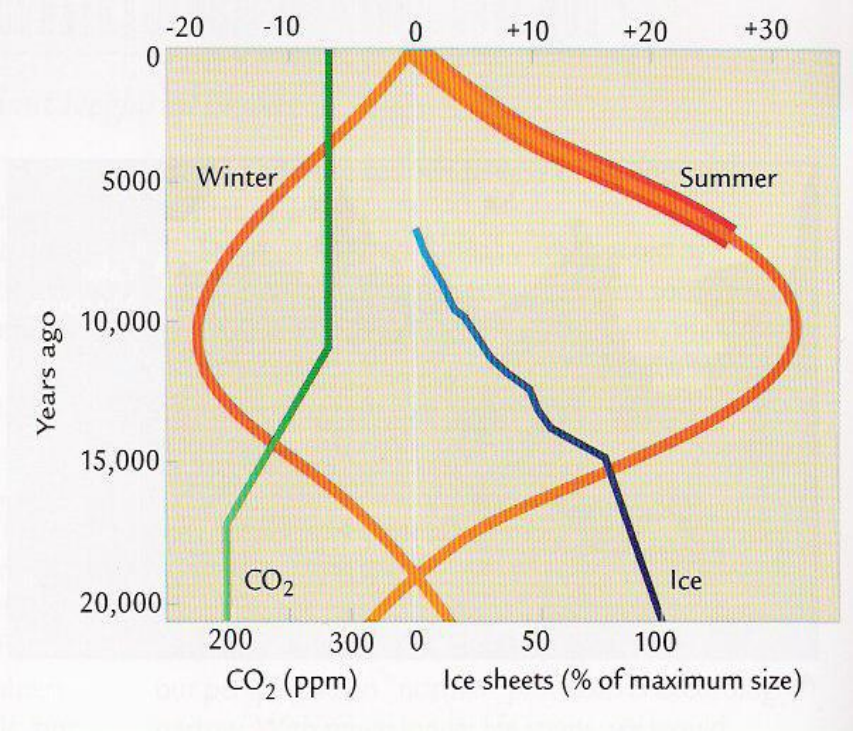

Figure 10. John Kutzback proposed a theory linking changes in insolation to the strength of monsoons over orbital time scale. Summer insolation was +30(W/m^2) higher than current levels around 10,000 ago, resulting in stronger monsoons. (Ruddiman, 2001)

Other evidence of strengthened monsoonal precipitation during the Early Holocene includes upwelling in the Arabian Sea (Tudhope et al., 1996). Stronger summer monsoons cause the deepening of the thermocline, thus decreasing the amount of aquatic nutrients above the thermocline and affecting the types of species living in that zone. Weaker summer monsoons cause the thermocline to become more shallow, and therefore increase aquatic nutrients and species that prefer such conditions. Upon their death, planktic organisms that inhabit near-surface waters leave shells that become incorporated into the ocean's seafloor. Sediment cores from the Western Arabian Sea showed a correlation between pollen, foraminifera, eolian dust grains, stable $\delta^{18}O$ and $\delta^{13}C$ isotopes and changes in monsoonal upwelling (Sarkar et al, 2000). Similar evidence comes from the $\delta^{18}O$ record of stalagmite H5 from Hoti cave in northern Oman (57˚21'E, 23˚05'N), which show a variation in $\delta^{18}O$ values in speleothem calcite that are associated with changing intensity of monsoon rainfall (Neff et al., 2001).

Since present climate conditions in northeastern Arabia and Kuwait favor deposition by eolian processes over fluvial processes, coupled with paleoclimatic observations that strongly suggest variation in rainfall and possible monsoonal activity in northeastern Arabia, I constructed a detailed stream network model for this area. The goal of this model is to identify any large channel features in northeastern Arabia and Kuwait. The presence of these channel-like features would support previous studies that suggested the dominance of more humid conditions during the early-mid Holocene. This new stream network model could then be used to select sites along those channel-like features, where detailed investigations of sediments and watersheds could be done to provide further information about the conditions of transport and deposition.

4.0 METHODOLOGY AND ANALYSIS

4.1 GIS and Arc Hydro

ArcGIS tools were used to identify possible stream networks in northeastern Arabia and Kuwait. The most widely used Geographic Information System (GIS) software packages are the Arc/Info and ArcView systems developed by ESRI in Redlands, California. Arc/Info was originally developed in 1980 to use a combination of vector data (points, lines, and polygons) with tabular attributes, and was later extended to include surface modeling using rasters and triangulated irregular networks (TIN). In the early 1990's, ArcView was initially developed as a simple viewing software for GIS data, but was later extended to support spatial analysis and modeling (Maidment, 2002) and is now the ArcGIS system. This system also includes spatial, geostatistical, and network analyst modules used in this research. Arc/Hydro is a geospatial and temporal data model for water resources that operates within the ArcGIS framework. It has an associated set of tools that populate the attributes of the features in the data framework, interconnect features in different data layers, and support hydrologic analysis (Maidment, 2002). It is also a data structure that supports hydrologic simulation models. Hydrologic simulation is accomplished by exchanging data between Arc/Hydro and an independent hydrologic model, by constructing a simulation model attached to Arc/Hydro using a dynamic linked library or by customizing the behavior of Arc/Hydro (Maidment, 2002).

4.2 Data Used in Analysis

A regional mosaic of the study area (Kuwait, NE Saudi Arabia, SE Iraq) was created with 30-meter resolution Shuttle Radar Topography Mission (SRTM) derived Digital Elevation Models (DEM) using ArcGIS 9.2 software. Eight tiles were used to create a 656,026 grid cells mosaic. In addition, Landsat data was acquired from the web site of the Global Land Cover Facility at the Institute for Advanced Computer Studies at the University of Maryland (http://glcf.umiacs.umd.edu/index.shtml). ArcCatalog was launched and each data set was examined for errors, such as cells that are missing data (no data). Since precipitation in that region occurs only during the winter months (Nov-April), only data taken during the dry summer months (May-Oct) were used in this project, as seasonal spring vegetation may affect the quality of the analysis and the landscape during the summer months is virtually vegetation-free. The lack of vegetation allows for more exposure of the terrain and landscape, thus improving the quality of the channel delineation process. Areas of no data, which were mainly over the Persian Gulf and outside of the study area, were removed before any analysis was performed. Pyramids, which are versions of a raster data set that are used to improve the drawing speed of raster layers (Ormsby et.al, 2001), were created for each data set.

The Cartesian map projection used was defined using the Define Projection function in the ArcMap's toolbox; the data was projected to Universal Transverse Mercator zone 38N in the WGS 1984 datum, with linear and spatial units in meters for this analysis (Fig. 11).

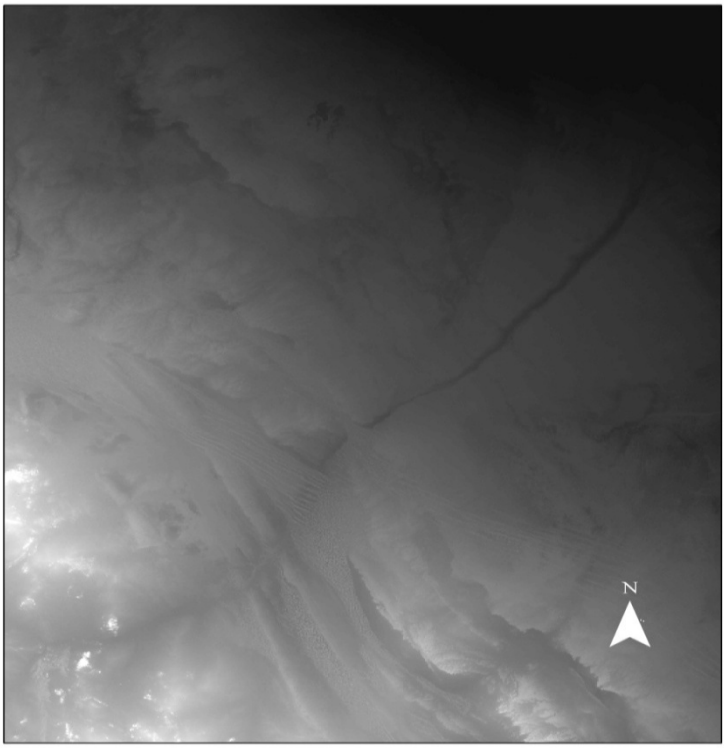

Figure 11. Regional mosaic of the study area created from SRTM derived Digital Elevation Models (DEM) (Data from http://glcf.umiacs.umd.edu/index.shtml)

Projected Coordinate System	WGS_1984_UTM_Zone_38N
Geographic Coordinate System	GCS_WGS_1984
Rows	997
Columns	658
Dataset Size	1.25 MB
Spatial Resolution (cell size)	16 meters

Table 2. Spatial properties of data used in analysis.

4.3 Hydrologic Modeling

Drainage divides and valley networks were identified using standard functions included within the ArcMap software. Specifically, the FLOWDIRECTION function was used to create a raster of flow direction from each cell to its steepest down slope neighbor. This

raster indicates the direction in which surface water will flow from one pixel to another by calculating the direction of steepest descent from each cell. The FLOWACCUMULATION function, in turn, was used to calculate an accumulation grid, which is a grid of accumulated flow to each downstream pixel. Accumulated flow is based upon the number of upstream pixels that contribute to each subsequent downstream pixel. ArcGIS accumulates the weight for all pixels in the grid that flow into each down slope cell. In general, pixels with zero flow are determined to be topographic highs whereas pixels with high accumulation denote areas of concentrated flow (i.e. used to determine the locations of stream channels). It is important to note that calculation of the accumulation grid assumes that all water is surface runoff and there is no interception, evaporation or infiltration. The WATERSHED function was used to delineate drainage divide and determine the contributing area above a set of cells in a raster. This was done using a quantitatively thorough and complex process based on the sink-fill depth, where points with low elevation surrounded by higher elevation pixels are identified then filled and assigned a new elevation value by averaging the surrounding pixels' elevations.

The STREAM DEFINITION function was used to compute a stream grid , where ArcMap assigned a value of "1" for all the cells in the input flow accumulation grid that have a value greater than the assigned threshold. All other cells in the Stream Grid were considered to contain no data, which is a standard ArcMap raster notation for a cell with an unidentified value. The assigned threshold was 5000 cells, which meant that all cells with a flow accumulation greater than 5000 cells were classified as stream cells, while the remaining cells were considered land surface draining to the steams. This threshold value is the typical value used in GIS hydro analyses, thus it was chosen for this analysis.

Finally, the STREAM SEGMENTATION function was used to create a grid of stream segments with a unique identification. Segments were designated as a head, or as a segment between two junctions. All cells in a particular segment have the same grid code that is specific to that segment. This step was necessary, as the grid codes were used in subsequent steps to define stream order. Modeled stream networks generated by ArcHydro identify a wide range of Strahler stream orders, ranging from first to fifth orders (Fig. 22). Specifically, fingertip tributaries are designated first order, and the junction of two streams of the same order (u) forms a channel segment of the next higher order (u+1). Stream orders are useful as order number is in general directly proportional to the size of the contributing watershed, channel dimensions, and discharge within the network (Strahler, 1964).

4.4 Analysis

Initial analysis of the DEM was carried out using the Hydrology tools within the Spatial Analyst tools in the ArcMap toolbox. Performing each step individually proved time consuming, and at times unsuccessful, as some of the operations were interrupted and an error messages were displayed. At the time, the precise cause of this failure was not determined, and it was believed to have been caused by the very large size of the DEM file. An alternative approach to this problem was creating a model using the model builder function in the ArcMap toolbox. This allowed for more flexibility and efficiency, as each operation is performed in an order specified by the user, thus saving time and allowing for better monitoring of each operation in progress (Fig. 12 a and b). Flow Direction, Sink, Fill and Watershed functions were added to the model in the previous

order. Once the model was run, the output of the Flow Direction function was added to a new model, where Flow Accumulation and Stream Order were performed.

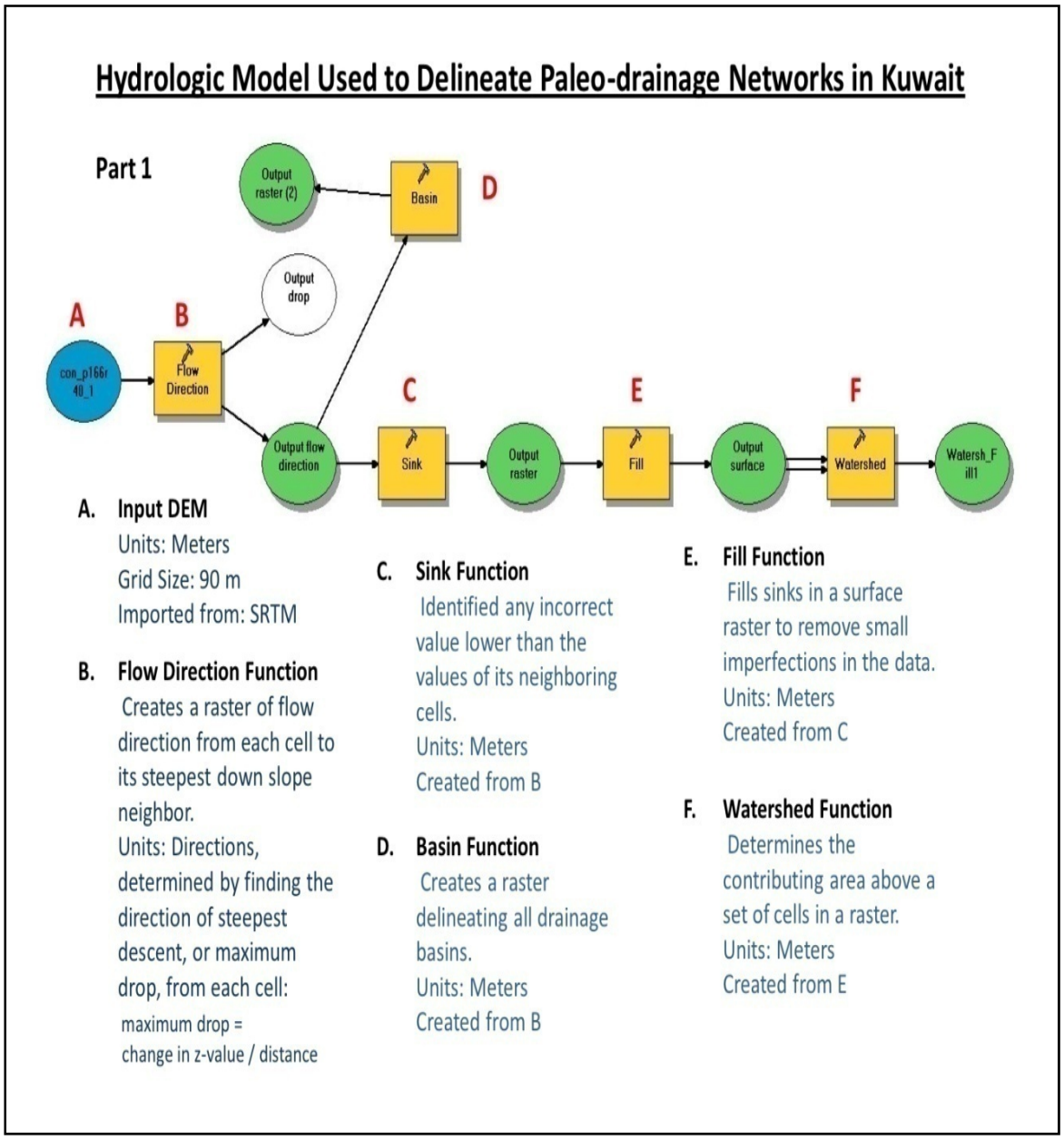

Figure 12a. Using the Model Builder function in the ArcMap toolbox, a model was created to analyze the DEM using hydrologic functions.

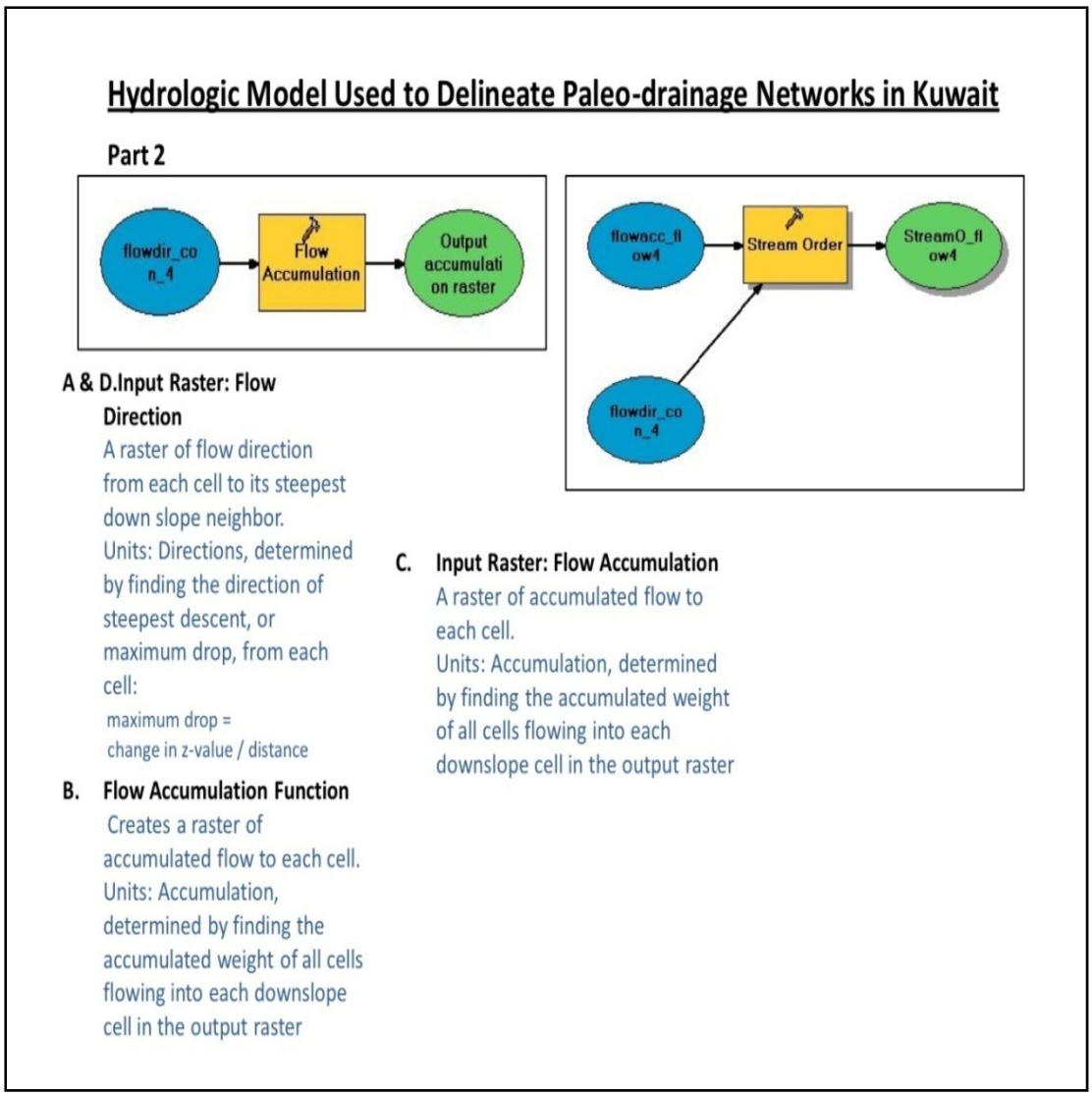

Figure 12b. Using the Model Builder function in the ArcMap toolbox, a model was created to analyze the DEM using hydrologic functions.

To validate this model and assess its accuracy, it was decided to use it on a previous study to test the model's results against the findings of that study. In 1997, topographic data sets of a river basin in San Antonio, Texas, were created by the U.S. Geological Survey (USGS) and the Texas Natural Resource Conservation Commission (TNRCC) to delineate drainage basins for streams and stream-sampling locations in Texas (USGS, 1997). Developing these data sets was done using Arc/Info (version 7.0.4) and provided in an ASCII grid format. Operations such as Flow Accumulation (Fig. 13 a) and Flow

Direction (Fig. 13 c) had been performed on these data sets and the results were verified for any errors. Since the purpose of this test was the validation of the model by comparing its results with the USGS's results, differences in climate and hydrology between Kuwait and San Antonio were not considered. Using the model builder function, the model was edited by replacing the DEM of the study area (Kuwait) with the DEM of a river basin in San Antonio, Texas. Since only Flow Direction and Flow Accumulation results were available in the Texas data sets, only these two operations were performed on the DEM of San Antonio. After running the model and loading the results as layers in the table of contents, they were compared to the results of USGS and TNRCC (Fig. 13 b and Fig. 13 d) and were found to be comparable, hence verifying the accuracy of the methodology and model (USGS, 1997).

The model was modified again by replacing the Texas DEM with the DEM of Kuwait, followed by the entire model being run on Kuwait's data. Although the Flow Direction and Basin operations were both successful, the Sink operation failed. Several attempts were made to solve this problem, including the creation of a new model and running every operation separately, but these attempts were unsuccessful. The large size of the data was thought to have been the cause of this failure. This created an obstacle, as subsequent operations cannot be performed before performing the Sink function. Therefore the model was abandoned and it was decided to use the Arc Hydro tools (version 1.3) as an alternative approach. Arc Hydro has six main menus that include different tools for modeling water resources. These menus include Terrain Preprocessing, Terrain Morphology, Watershed Processing, Attribute Tools, Network Tools, and Buttons and Tools.

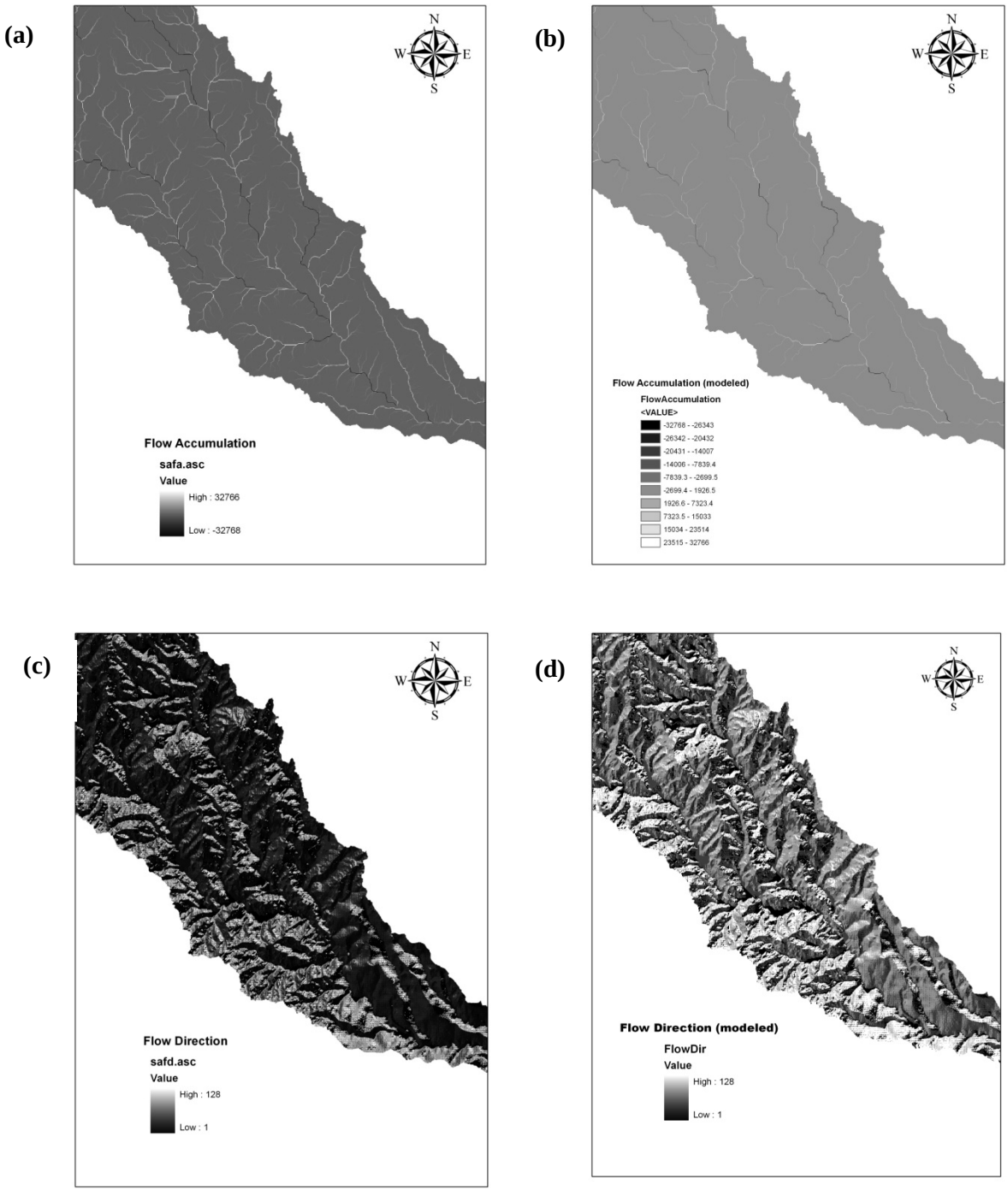

Figure 13. (a) Flow Accumulation data for the San Antonio, Texas area created by USGS and TNRCC. (b) Modeled Flow Accumulation for the same San Antonio area. (c) Flow Direction data for the San Antonio area created by USGS and TNRCC. (d) Modeled Flow Direction for the same San Antonio area.

Analyzing the DEM began by performing a Sink Prescreening, which screens the potential sinks in the input DEM. The Sink Prescreening step failed, and this led to extensive examination of the DEM's parameters. Consequently, a discrepancy between the DEM's units (degrees) and the units used in the Sink analysis (meters) was discovered, causing all failures that were initially attributed to the size of the data. Thus, the DEM was re-projected using the Define Projection function, and its units were changed to meters. Subsequently, the Sink Prescreening function was tested to verify whether re-projecting the DEM solved the problem, and it was a success.

To validate these steps and correct for any errors, they were performed on the Texas data created by the USGS, which was previously used to validate the model created at the beginning of this analysis (Fig. 12a, 12b). The functions used to analyze the Texas data were Sink Prescreening, Fill Sinks, Flow Direction, and Flow Accumulation, respectively. Since the Texas data did not contain any Sink Prescreening or Fill Sinks layers, only the Flow Direction and Accumulation layers were evaluated against the USGS-produced Texas data. The results were comparable (Fig. 14) thus validating the functions used for analysis and their sequence.

The Sink Prescreening function was performed (Fig. 15), and this was followed by the Fill Sinks function, which eliminates any problems associated with any cells that might be surrounded by higher elevation cells, consequently trapping water in that lower elevation sink and preventing flow. To compute the flow direction (Fig. 16) for a given grid the Flow Direction function was used, followed by the Flow Accumulation function (Fig. 17), which creates a grid that records the number of cells that drain into an individual cell in the grid. Using the Flow Accumulation grid, the Stream Definition

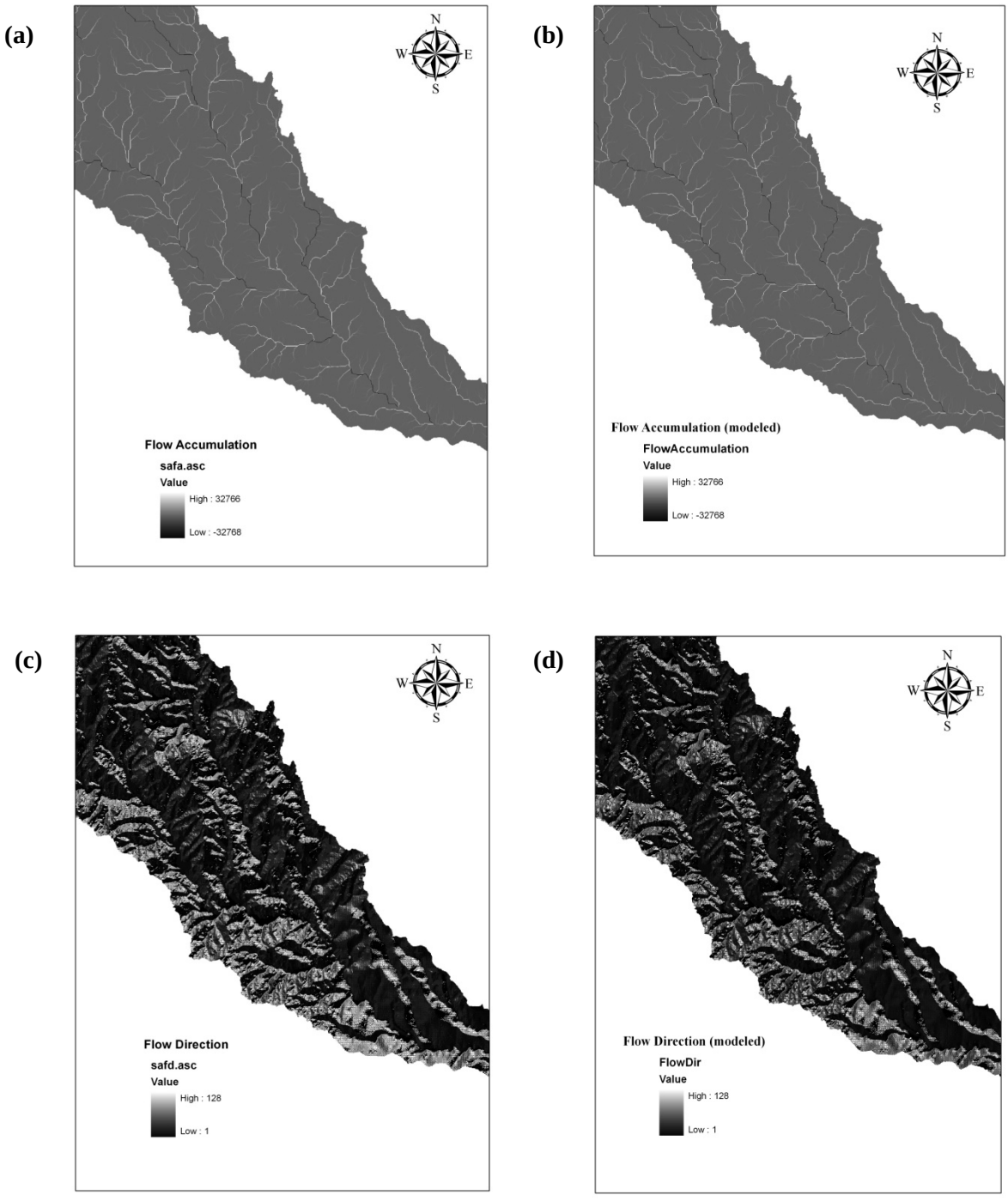

Figure 14. (a) Flow Accumulation data for the San Antonio, Texas area created by USGS and TNRCC. (b) Modeled Flow Accumulation for the same San Antonio area. (c) Flow Direction data for the San Antonio area created by USGS and TNRCC. (d) Modeled Flow Direction for the same San Antonio area.

function was performed to compute a stream grid that contains a value of "1" for all the cells in the input flow accumulation grid that have a value greater than the given threshold (5000 was the set threshold), and "no data" for all other cells. The Stream Segmentation function, which created a grid of stream segments that have a unique identification based on segments designated as head or as a segment between two junctions, was applied to the flow direction and stream definition grids. Finally, the stream order function was used to assign a numeric order to segments of a raster representing branches of a linear network (Fig. 18). There are two methods for assigning stream order; the STRAHLER and the SHREVE. The STRAHLER method was used because it is the most common method of ordering.

In the STRAHLER order method, all links with no tributaries are assigned an order of one and are referred to as first order (Strahler, 1964). When two first-order links intersect, the down slope link is assigned an order of two. When two second-order links intersect, the down slope link is assigned an order of three and so on. When two links of the same order intersect, the order increases (ESRI).

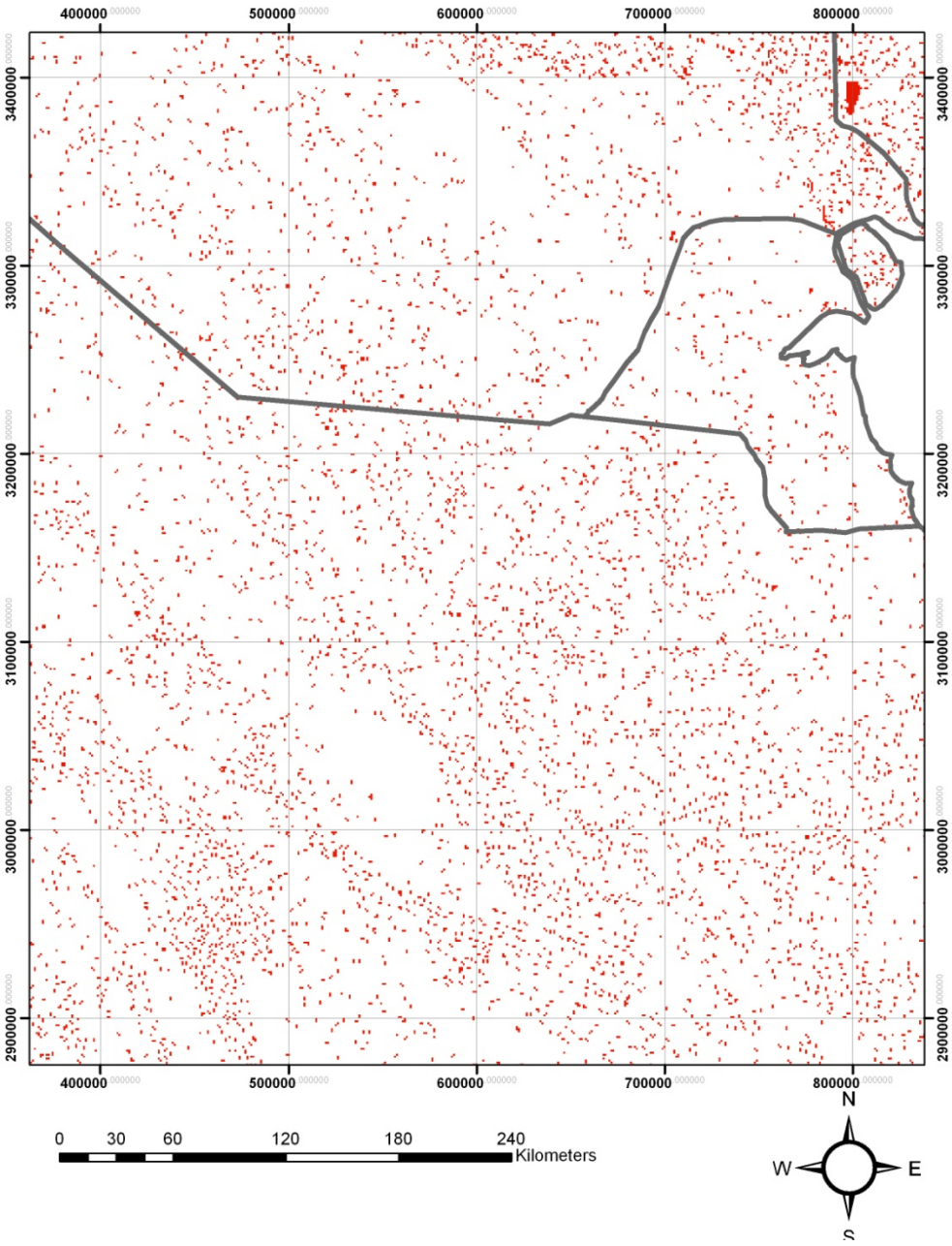

Figure 15. The Sink Prescreening function prescreens the DEM for potential sinks.

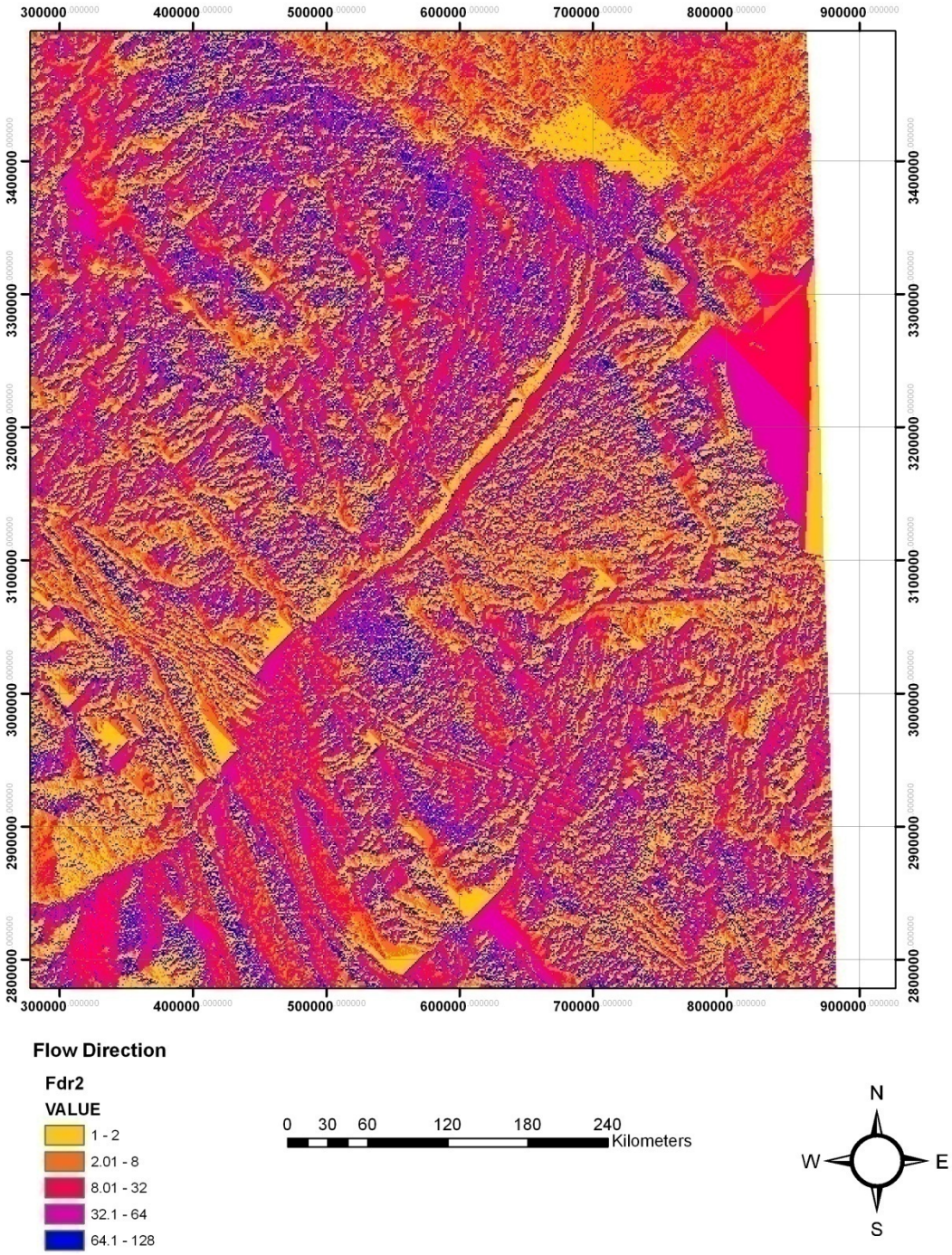

Figure 16. The Flow Direction function creates a raster of flow direction from each cell to its steepest down slope neighbor.

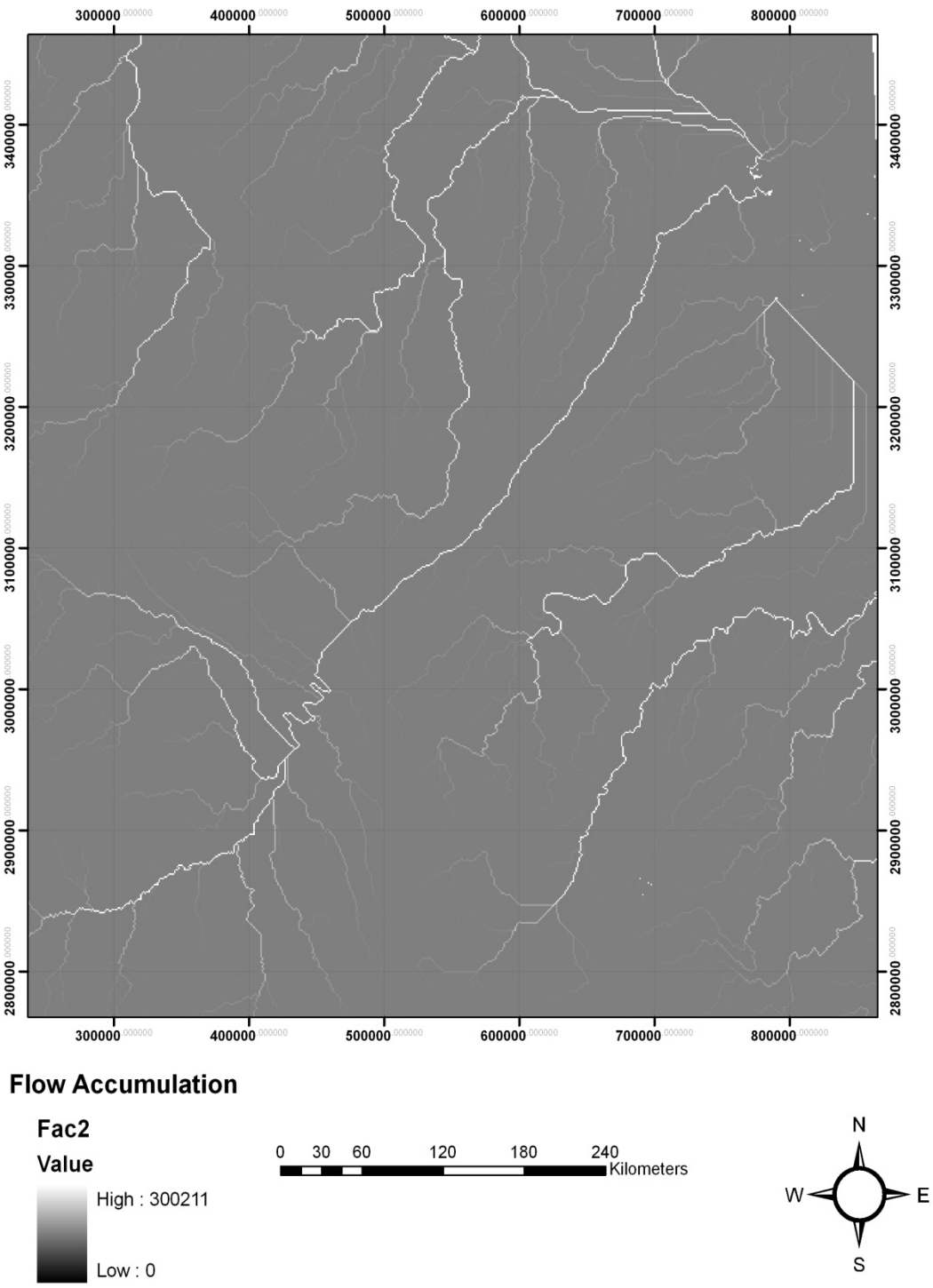

Figure 17. The Flow Accumulation function calculates an accumulation grid that contains the accumulated number of cells upstream of a cell.

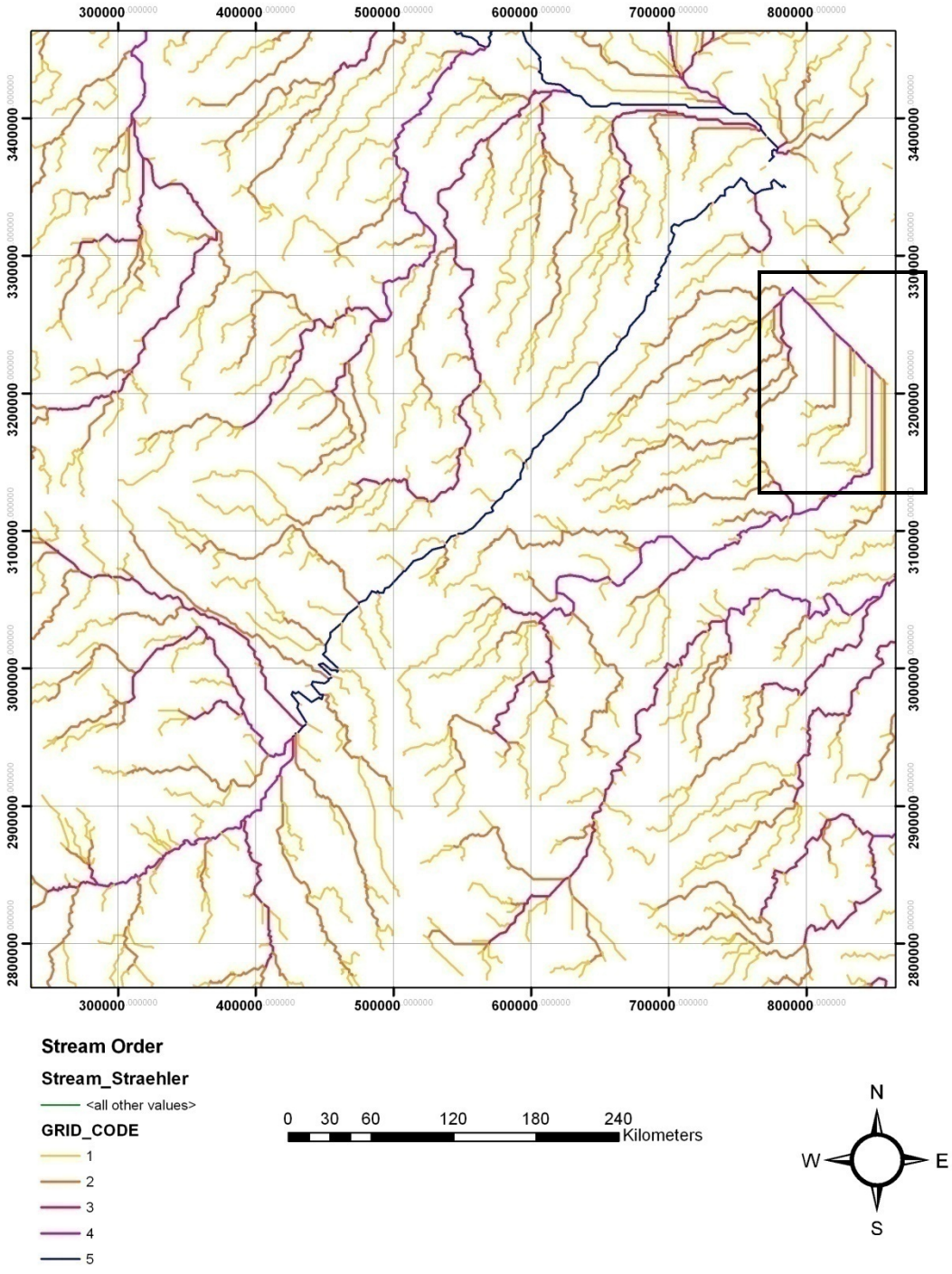

Figure 18. The Stream Order function assigns a numeric order to segments of a raster representing branches of a linear network. Streams that appear to flow over the surface of the Persian Gulf (see box above) will be removed in the next step.

To remove any streams that appear to flow over the Persian Gulf's surface, an ESRI-produced layer for country boundaries (interior and maritime) was added to the data display and used to extract streams that flow beyond Kuwait's coastal boundaries. This was performed with the Clip function, using the Stream Order grid as the Input Feature and the Country Outlines layer as the Clip Feature. By performing the clip function, a high spatial resolution stream network was completed (Fig. 19). An additional step was later added to the analysis, and it involved downloading Bathymetric data for the Persian Gulf, and examining if any of the modeled streams continued to flow on the bottom of the Persian Gulf. Unfortunately, the only available free Bathymetric data available for that region (National Geophysical Data Center) had a spatial resolution of 1 Km per pixel, which was too coarse in comparison to the data used in this analysis, which had a resolution of 16 meters per pixel (Fig. 20). Consequently, extending the analysis to the bottom of the Persian Gulf was suspended until other data sets with a higher spatial resolution were available.

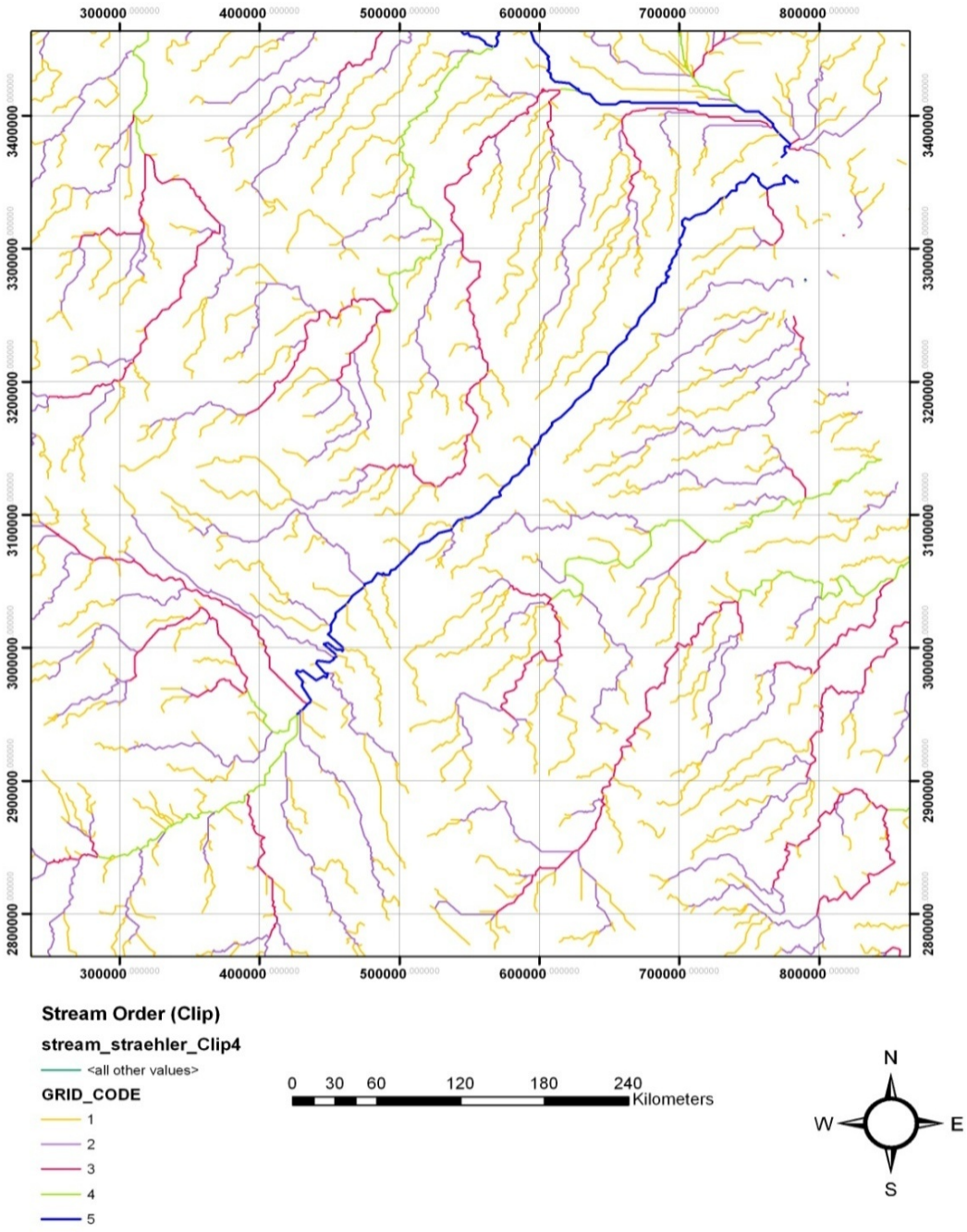

Figure 19. The Clip function removed any streams that flow over the Persian Gulf's surface. A "countries outline" layer was used as the Clip feature.

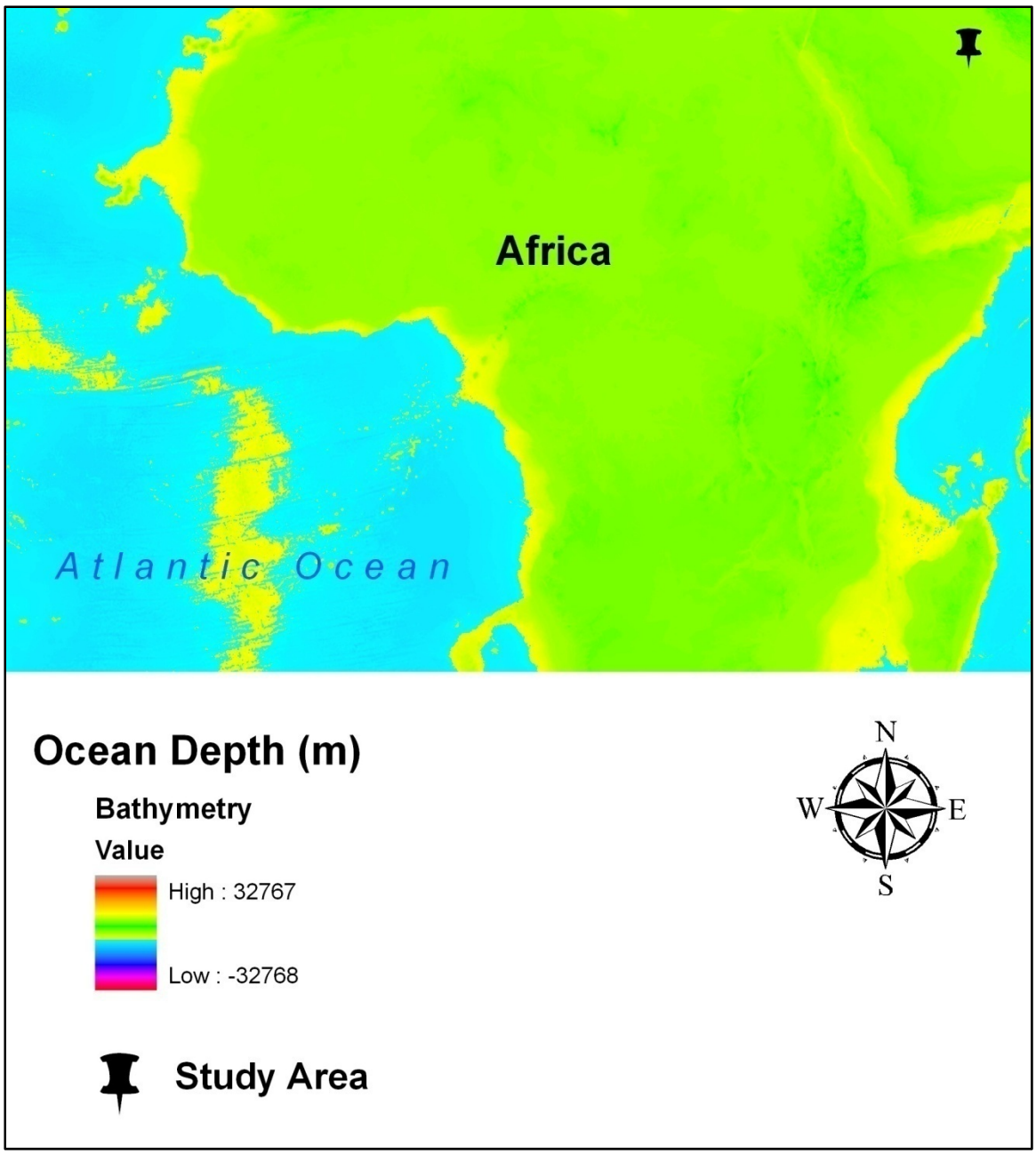

Figure 20. Because of the Bathymetric data's coarse resolution, extending the stream network modeling and analysis into the bottom of the Persian Gulf was not possible. Although the vertical (Z-value) units of this data are in meters, spatial resolution was 1 Km per pixel, which is very low when compared to the study area's terrestrial resolution of 16 meters per pixel.

5.0 RESULTS AND DISCUSSION

Regional topography has played a significant role in the morphometric characteristics of the modeled drainage basins (Fig. 21). The modeled stream basins are generally dendritic in their drainage pattern, although several exhibit a parallel pattern. A dendritic drainage pattern is often associated with areas of gentle regional slopes, whereas a parallel pattern is associated with areas of moderate to steep slopes (Ritter, 2002).

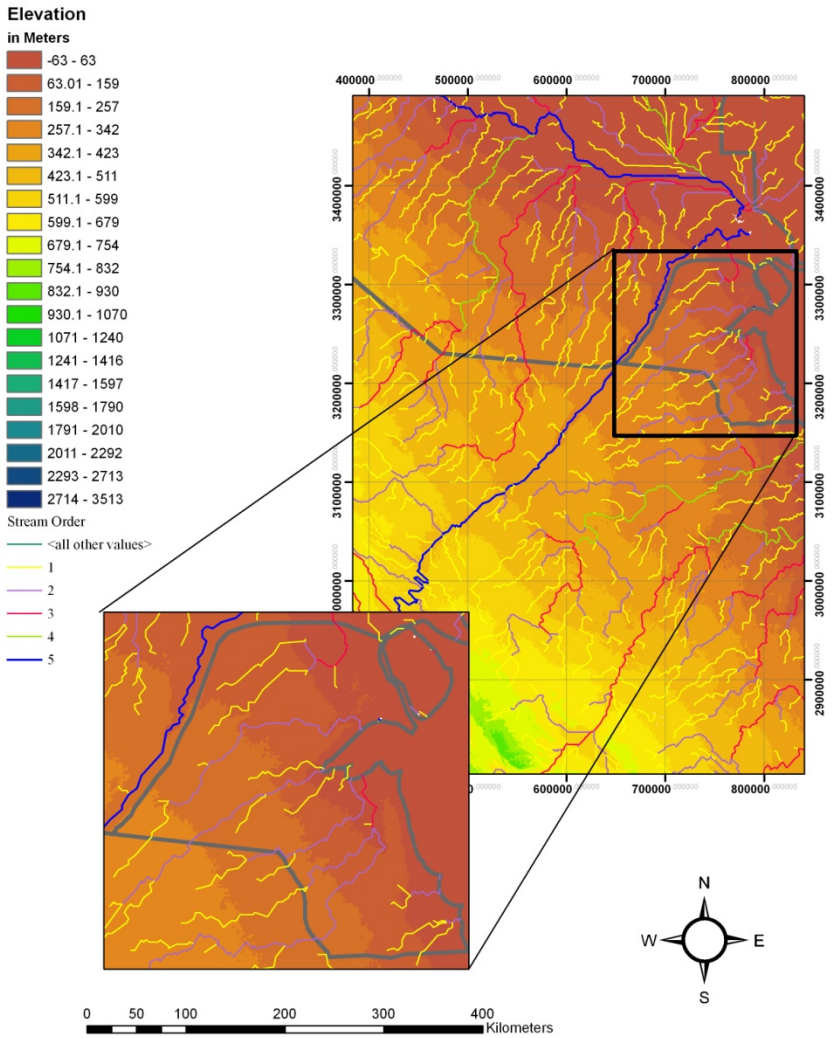

Figure 21. Regional topography is key to the characteristics of modeled drainage basins. As elevation increases from NE to SW, the general direction of stream flow is towards the NE.

The general direction of flow is towards the NE, which is also the direction of elevation decrease. One hundred sixty eight (168) fourth order streams merge to form nine main fourth order stream features (Table 3) (Fig. 22). Similarly, seventy six (76) fifth order streams merge to form two prominent and large stream features that dominate the area (Fig. 23). The first stream is located in Iraq, and it echoes the Euphrates River. Since this river is outside of the study area, it was therefore not analyzed. The second stream begins in NE Saudi Arabia and flows towards the NE along the Iraqi-Kuwaiti borders. Using the Measure tool in ArcMap, this stream was estimated to be ~170 Km long. Despite both streams being identified by ArcMap as fifth order streams, the stream in the study area (NE Saudi Arabia and Kuwait) is dry at present. This suggests that this stream may have been active at some point when precipitation was higher than evaporation, enabling the generation of significant surface runoff. These conditions are present in Southern Oman, where ephemeral streams form annually as a result of monsoonal rainfall.

Stream Order	*Count*	*Area*
First	1285	19027701
Second	641	9424640
Third	332	4552505
Fourth	168	2035984
Fifth	76	1157008
Total	*2502*	*36197841*

Table. 3. Number of classified stream segments and their area in Sq. Km.

Arid regions and deserts in particular are dominated by wind-driven (eolian) sediment transport and deposition processes. However, water may also play a role in sediment movement, although this is a much smaller role due to the sporadic nature of rainfall in these regions. Eolian deposits typically consist of fine sediments (about 0.05 mm), although coarser sediments can be transported and deposited through traction and saltation by higher winds (Boggs, 2006). In contrast, regions where fluvial (water-driven) processes are dominant have deposits that consist of sand and gravel, with sorting of those sediments ranging from moderate to poor (Boggs, 2006). Mud deposits are also present, forming during low flow periods. Al-Dabi *et al.* (1996) located shallow basins in the western and northwestern parts of Kuwait's desert. Gypsum and other evaporitic minerals were found at the surface of the playa lakes. They concluded that these playa lakes were relic features of wetter climate in the past. Another study by Al-Sulaimi *et al* (1995) examined two locations in northern and western Kuwait, where low-lying areas and depressions were covered with desert-plain deposits. They concluded that these deposits formed as a sheet wash of reworked material by fluvial processes during a wetter period.

Semi-arid and arid regions often experience a rapid decrease in the volume of flood flows due to rapid infiltration into the dry and porous substrata (Al-Sulaimi *et al.*, 1995). If the GIS-generated stream networks were active in the past, large amounts of water would have infiltrated into the desert floor and developed into ground water. Presently, ground water in Kuwait is considered fossil water, as current climatic conditions do not allow for sufficient replenishment and maintenance of the water table in that region (Mukhopadhyay *et al.*, 1996). The formation of ground water aquifers in northeastern

Arabia and Kuwait could therefore be attributed to wetter periods that initiated and maintained stream networks in the area, and later infiltrated into the dry and porous surface of the desert. Isotopic analyses (^{14}C) of the Kuwait Group aquifer water suggested an age of 7,000-10,000 years (Mukhopadhyay *et al.*, 1996), which coincides with the last northward-incursion of the summer monsoon into northern Arabia. Therefore, it is possible that a stronger summer monsoon caused the formation of active stream networks in northeastern Arabia and Kuwait, which carved the surface and led to the formation of the Kuwait Group aquifer.

Future research that focuses on the source of precipitation is recommended to determine the accuracy of the northward incursion of the summer monsoon theory. Possible sites where further field investigation should be performed are listed in Table 3. These sites were chosen purely due to their location at the beginning, middle, and end of the modeled stream channel that is within Saudi Arabia, and additional sites along this channel may also be chosen.

	Coordinates (Meters)	*Coordinates (degrees, minutes, seconds)*
Site 1	426,934.940 2,949,938.804	44°15'56.6"E 26°40'6.9"N
Site 2	577,338.287 3,123,093.503	45°47'17.716"E 28°13'53.224"N
Site 3	634,091.108 3,192,737.083	46°22'29.013"E 28°51'19.287"N

Table. 4. Locations of possible sites for future field investigation.

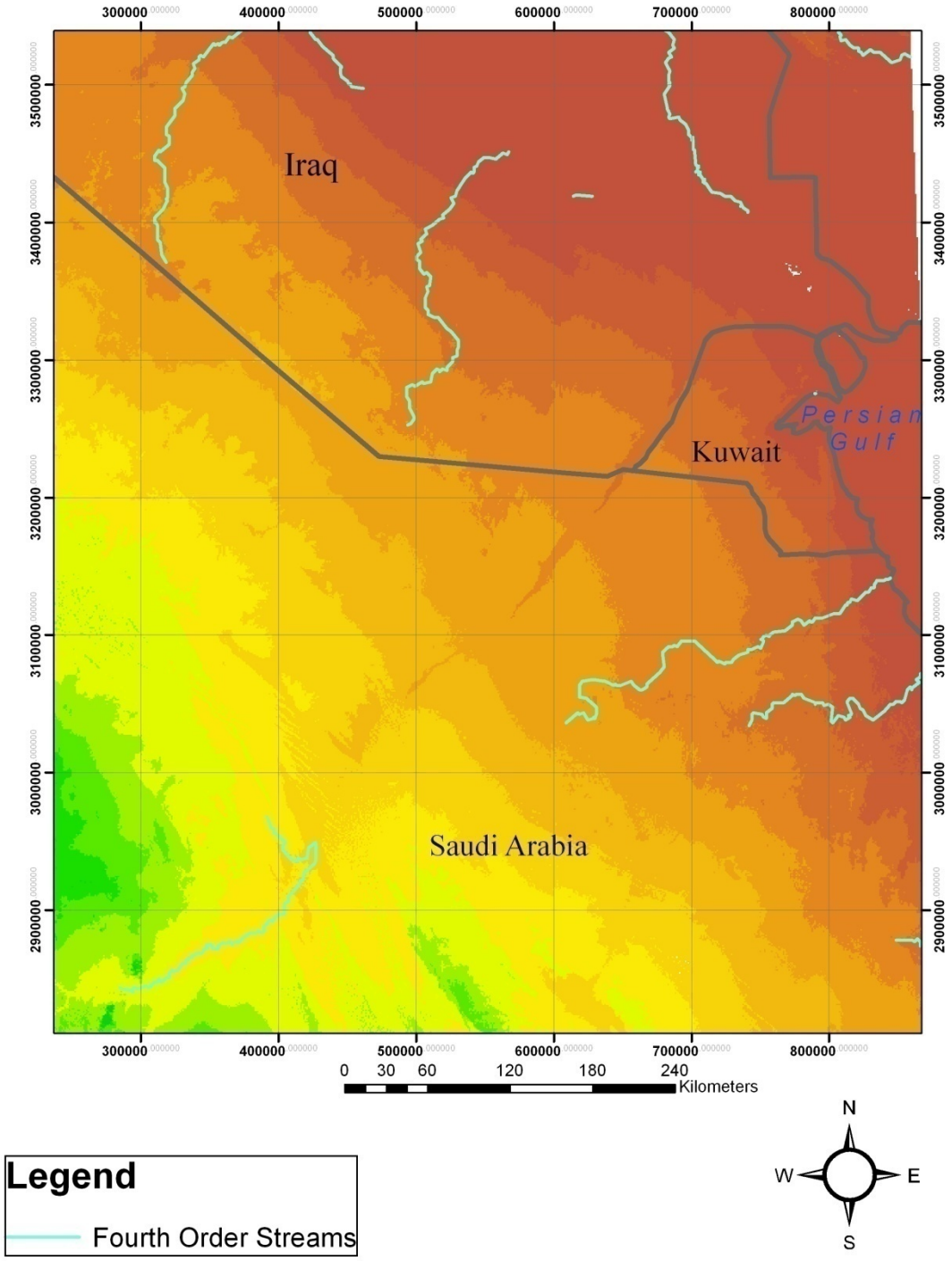

Figure 22. One hundred sixty eight (168) fourth order streams merge to form nine (9) main fourth order stream features.

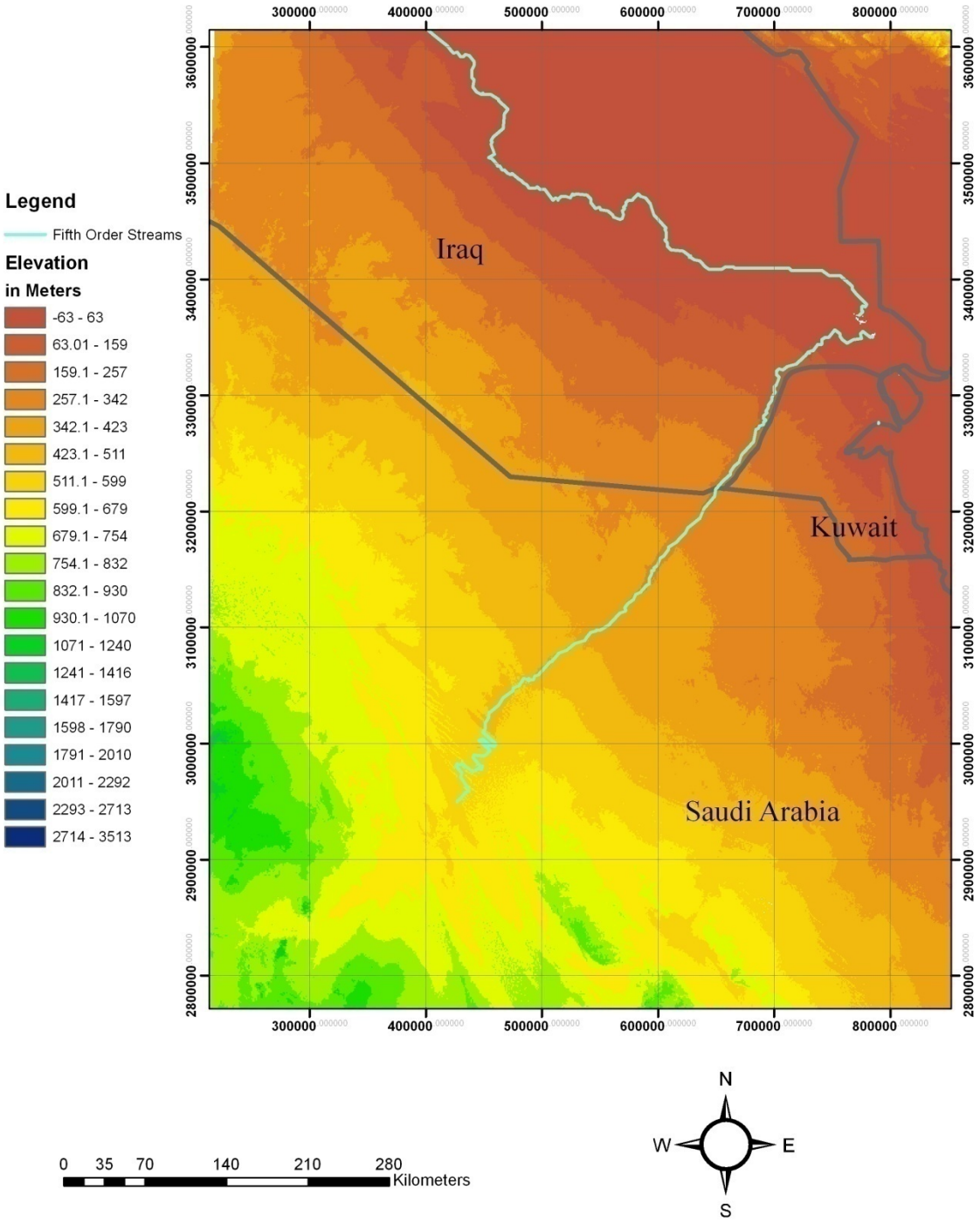

Figure 23. Seventy six (76) fifth order streams merge to form two (2) main fifth order streams. The northern stream represents the Euphrates River in Iraq.

6.0 CONCLUSION

Two thousand five hundred and two (2502) stream segments were identified in the study area, with seventy six (76) segments representing fifth order stream segments. These fifth order stream segments form two prominent stream features, with the northern stream representing the Euphrates River in Iraq. The southern stream feature is dry at present, suggesting that it might have been an active stream in the past. Examining the lithology and stratigraphy of an area usually leads to better understanding of the environment of deposition and the processes involved. Therefore, it is only possible to make assumptions about the feature identified as a fifth order stream by ArcHydro, as field investigation of the deposits along this stream is needed to reveal whether this feature is indeed a paleochannel created by fluvial processes during a wetter period. Furthermore, similar field investigation should be performed on the deposits created by Monsoonal ephemeral streams in Southern Oman and the deposits of the Euphrates River in Iraq, as this could reveal more about the nature of this stream and whether it was perennial or ephemeral. Future research that focuses on the source of precipitation is recommended to determine the accuracy of the northward incursion of the summer monsoon theory and or any other sources of moisture, such as Mediterranean cyclonic winter rainfall. Considering the political and security situations in Iraq, it is unlikely that any field work can be performed along the Iraqi-Kuwaiti border in the near future, thus field studies should be completed on the southern sections of this feature in Saudi Arabia.

BIBLIOGRAPHY

Al-Dabi, H., Koch, M., Al-Sarawi, M., El-Baz, F. 1996. Evolution of sand dune patterns in space and time in north-western Kuwait using Landsat images. *Journal of Arid Environments* 36: 15-24.

Al-Sulaimi, J., Pitty, A.F. 1995. Origin and depositional model of Wadi Al-Batin and its associated alluvial fan, Saudi Arabia and Kuwait. *Sedimentary Geology* 97: 203-229.

Al-Sulaimi, J., Khalaf, F., Mukhopadhyay, A. 1997. Geomorphological analysis of paleo drainage systems and their environmental implications in the desert of Kuwait. *Environmental Geology* 29 (1/2): 94-111.

Al-Sulaimi, J., Khalaf, F., Mukhopadhyay, A. 2000. An Overview of the Surface and Near-surface Geology, Geomorphology and Natural Resources of Kuwait. *Earth Science Reviews* 50: 227-267.

American Meteorological Society. http://www.ametsoc.org/amsedu/WES/glossary.html

Boggs, Sam JR. 2006. *Principles of Sedimentology and Stratigraphy*. Upper Saddle River: Pearson.

deMenocal, P., Ortiz, J., Guilderson, T., Adkins, J., Sarnthein, M., Baker, L., Yarusinsky, M. 2000. Abrupt onset and termination of the African Humid Period: rapid climate responses to gradual insolation forcing. *Quaternary Science Reviews* 19: 247-361.

Edgell, Stewart H. 2006. *Arabian Deserts*. Dordrecht: Springer.

Environmental Systems Research Institute (ESRI). http://www.esri.com

Fischer, H., Kumke, T., Lohmann, G., Flöser, G., Miller, H., Von Storch, H., Negendank, J. eds. 2004. *The Climate in Historical Times*. New York: Springer.

Global Land Cover Facility. http://glcf.umiacs.umd.edu/index.shtml.

Hecht, Alan D. 1985. *Paleoclimate Analysis and Modeling*. Wiley-Interscience: New York.

Kutzbach, John E. 1981. Monsoon Climate of the Early Holocene: Climate Experiment with the Earth's Orbital Parameters for 9000 Years Ago. *Science* 214: 59-61.

Kutzbach, J., Street-Perrott, F.A. 1985. Milankovitch Forcing of Fluctuations in the Level of Tropical Lakes from 18 to 0 Kyr B.P. *Nature* 317: 130-134.

Maidment, David R. ed. 2002. *Arc Hydro GIS for Water Resources.* Redlands: ESRI Press.

Mukhopadhyay, A., Al-Sulaimi, J., Al-Awadi, E., Al-Ruwaih, F. 1996. An overview of the Tertiary geology and hydrogeology of the northern part of the Arabian Gulf region with special reference to Kuwait. *Earth Science Reviews* 40: 259-295.

National Geophysical Data Center. http://www.ngdc.noaa.gov/mgg/global/global.html

National Oceanic and Atmospheric Administration.
http://www.srh.noaa.gov/jetstream//global/images/jetstream3.jpg

Neff, U., Burns, S., Mangini, A., Mudelsee, M., Fleitmann, D. 2001. Strong coherence between solar variability and the monsoon in Oman between 9 and 6 kyr ago. *Nature* 411: 290-292.

Ormsby, T., Napoleon, E., Burke, R., Groessl, C., Feaster, L. 2001. *Getting to Know ArcGis Desktop.* Redlands: ESRI Press.

Paeth, H., Hense, A., Glowienka-Hense, R., Voss, R., Cubasch, U. 1999. The North Atlantic Oscillation as an indicator for Greenhouse-gas induced regional climate change. *Clim Dyn* 15:953-960.

Ritter, D., Kochel, C., Miller, J. 2002. *Process Geomorphology*. New York: McGraw-Hill.

Ruddiman, William F. 2001. *Earth's Climate Past and Future*. New York: W.H. Freeman and Company.

Sarkar, A., Ramesh, R., Somayajulu, B.L.K., Agnihotri, R., Jull, A.J.T., Burr, G.S. 2000. High Resolution Holocene monsoon record from the eastern Arabian Sea. *Earth and Planetary Science Letters* 177: 209-218.

Strahler, A.N. (1964), Part II. Quantitative geomorphology of drainage basins and channel networks, in *Handbook of Applied Hydrology: A Compendium of Water-resource Technology*, pp. 39-76, V.T. Chow, ed., McGraw-Hill, Inc.

Tudhope, A., Lea, D., Shimmield, G., Chilcott, C., Head, S. 1996. Monsoon Climate and Arabian Sea Coastal Upwelling Recorded in Massive Corals from Southern Oman. *PALIOS* 11: 347-361.

U.S. Geological Survey. 1997. Topographic Data Sets for Texas By River Basin. DOCS CD. 97-354.

Weyhenmeyer, C., Burns, S., Waber, H., Aeschbach-Hertig, W., Kipfer, R., Loosli, H., Matter, A. 2000. Cool Glacial Temperatures and Changes in Moisture Souce Recorded in Oman Groundwaters. *Science* 287: 842-845.